

of the placenta provided confirmatory evidence concerning the COD; provided new information and COD; or did not provide additional information regarding the COD.

Results: During the 21-year period examined, 458 stillborn autopsies were performed; 388 of these autopsies revealed structurally normal fetuses (84.7%). Of the structurally normal fetal autopsies, 94 cases (24%) were performed prior to the policy institution and 294 after. Comparing the frequency of placental examination and COD determination before and after the policy (1992), we demonstrated that the percentage of placental examinations increased from 42.2±5.3 % (1987-1991) to 92.1±2.1 % (1992-2007), and the frequency of COD determination increased from 38.5±7 % to 79.5±3.2 % (P<0.0001). The placental examination provided confirmatory evidence in 24.6 %, new diagnostic information and COD in 44.7 % and no additional information in 30.7 %. However, in those that did not yield any additional information, COD was identified from the clinical history in 27 % and in the remainder, several common causes of intrauterine demise, such as intrauterine infection or villitis of unknown etiology, were excluded.

Conclusions: The cause of death in structurally normal intrauterine fetal demise cases is more likely to be identified if routine pathologic examination of the placenta is performed.

Bone & Soft Tissue

34 Novel Kinase Mutations in *KDR/VEGFR2*, *TIE1*, and *SNRK* in Angiosarcoma (AS) Patients

CR Antonescu, A Yoshida, NP Agaram, NE Chang, RG Maki. Memorial Sloan-Kettering Cancer Ctr, New York, NY.

Background: The pathogenesis of AS is not well understood and anecdotal evidence suggests that at least a subset of patients respond to VEGFR targeted therapy. However no potential molecular candidates have been identified so far to guide a more specific therapeutic intervention.

Design: Forty-two samples from 39 AS patients were included in the analysis. A HG U133A Affymetrix platform (22,000 transcripts) was used to mine the gene expression of 22 AS, compared to a control group of a well-characterized set of 45 soft tissue sarcomas. Candidate kinase genes overexpressed in AS compared to other sarcoma types were selected for full-length sequencing using a high throughput mutational profiling. Identified mutations were then validated by direct sequencing in matched tumor/normal samples. Selected genes were also validated at the protein level by IHC in an AS tissue microarray.

Results: Unsupervised clustering showed that AS formed a tight genomic group distinct from all other sarcoma types. Its distinctive expression profile included overexpression of a number of kinase genes, such as *TIE1*, *KDR/VEGFR2*, *SNRK*, *TEK*, and *FLT1/VEGFR1*. Full-sequencing of these 5 genes identified mutations in 10 (25%) patients, including *KDR* (6/10), *TIE1* (2/10) and *SNRK* (2/10). *KDR* mutations were identified only in AS located in the breast/chest wall, with or without radiation exposure. However, overall kinase mutations were seen more often in radiation-associated tumors (40% vs 18%). The 2 patients with lymphedema-associated tumors lacked mutations. The presence of *KDR* mutations correlated with the protein expression by IHC in the AS TMA, being 3+ positive in all 6 *KDR*-mutated tumors, while negative in the *TIE1* or *SNRK*-mutated AS.

Conclusions: We identified novel mutations in *KDR*, *TIE1* and *SNRK* in 25% of AS patients. These findings open new ground for understanding the AS pathogenesis and will be instrumental in identifying the subset of patients responding to VEGFR specific targeting. Furthermore, *KDR* immunoreactivity, which was seen in 60% of AS, may be useful as a screening method for potential kinase mutations.

35 RT-PCR Analysis for FGF23 Using Paraffin Sections in the Diagnosis of Phosphaturic Mesenchymal Tumors with and without Known Tumor Induced Osteomalacia: A Study of 27 Cases

A Bahrami, RV Lloyd, SW Weiss, E Montgomery, AE Horvai, L Jin, CY Inwards, AL Folpe. Mayo Clinic, Rochester, MN; Emory University, Atlanta, GA; Johns Hopkins Medical Institutions, Baltimore, MD; UCSF, San Francisco, CA.

Background: Phosphaturic mesenchymal tumors of the mixed connective tissue type (PMTMCT) are extremely rare, histologically distinctive neoplasms which cause tumor-induced osteomalacia (TIO) in most cases through elaboration of a phosphaturic hormone, fibroblast growth factor-23 (FGF-23). Rarely, identical tumors without known TIO may be seen. We studied a large group of PMTMCT for expression of FGF-23, utilizing a novel RT-PCR assay for FGF-23 in formalin-fixed, paraffin-embedded (FFPE) tissues.

Design: 27 PMTMCT (14 with, 13 w/o TIO) and 11 non-PMTMCT (6 chondromyxoid fibromas (CMF), 2 chondroblastomas, 1 SFT, 1 osteosarcoma, 1 paraganglioma) were retrieved. Total RNA was extracted from FFPE sections for RT-PCR analysis. FGF23 was amplified using three sets of primers that spanned the intron/exon boundaries to amplify the three exons of FGF23 gene (140 bp, 125bp, and 175 bp). The housekeeping gene phosphoglycerokinase (PGK, 189bp) was co-amplified to check RNA quality. Products were visualized by Agilent 2100 Bioanalyzer, Agilent DNA 1000 Kit and DNA chips. 2 PMTMCT with TIO, 3 PMTMCT without TIO and 5 non-PMTMCT lacked a positive PGK control and were excluded.

Results: 11 of 12 (92%) PMTMCT with known TIO were FGF23-positive. 9 of 13 (69%) PMTMCT without known TIO were FGF23-positive. One CMF was positive; all other non-PMTMCT were negative.

Conclusions: We conclude that RT-PCR for FGF-23 is a sensitive and specific means of confirming the diagnosis of PMTMCT both in patients with and without TIO. FGF-23 gene expression was present in >90% of PMTMCT with known TIO, confirming the role of FGF-23 in this syndrome. Rare FGF-23-negative PMTMCT with known TIO

likely express other phosphaturic hormones (e.g., frizzled related protein 4). Our finding of expression of FGF-23 in 69% of histologically identical tumors without known TIO confirms the reproducibility of the diagnosis of PMTMCT, even in the absence of known phosphaturia. FGF-23-positive PMTMCT without known TIO were likely excised prior to becoming symptomatic. The exact nature of FGF-23-negative putative PMTMCT without TIO is unclear, although histological re-review did not suggest alternative diagnoses. Ongoing study of additional non-PMTMCT should further establish the frequency of FGF-23 expression in other tumor types.

36 Characterization of CXCR4 Expression in Chondrosarcoma of Bone

S Bai, D Wang, MJ Klein, GP Siegal. University of Alabama at Birmingham, Birmingham, AL.

Background: The CXCR4/SDF-1 system has been found to strongly correlate with neoplastic progression leading to metastases in a number of tumors including those of prostate, skin, breast, muscle, and bone. Increased CXCR4 mRNA expression in osteosarcoma tumor samples has previously been shown to correlate with reduced overall survival and with the presence of metastases at diagnosis. Excluding hematologic malignancies, chondrosarcoma (CS) of bone is the most common primary malignant tumor of bone, in adults in the U.S. Whether CXCR4 is detectable in CS and whether CXCR4 expression level correlates with CS grade, progression, and prognosis was the subject of this study.

Design: Archived materials from 22 CS samples banked between 2001 and 2006 were retrieved. All the slides were reviewed microscopically to confirm the initial diagnosis. The pathological features of the tumors were evaluated. Immunohistochemistry using monoclonal anti-CXCR4 antibody (R&D Systems) was performed on formalin-fixed, paraffin-embedded tissue sections and analyzed by histomorphometric techniques. Invasive ductal carcinoma of the breast was used as the positive control. All controls reacted appropriately.

Results: There were 14 high-grade (Grade II-III) CSs and 8 low-grade (Grade I) CSs. The 14 high-grade CS samples were derived from 12 patients. A single sample was provided by 18 patients and 2 samples were available from the remaining 2 patients. Of the study cohort, 10 were males and 10 females, ranging in age from 24 to 80 years. Follow-up ranged from 3 to 84 months. Essentially, all CS cells stained for CXCR4. However, the percentage of the positive area in the selected tumor fields between these two groups was significantly different, with significantly greater positivity in the high-grade tumors (p<0.001). More interestingly, the staining intensity of the CXCR4 between the two groups was also significantly different. There was a higher staining intensity in high grade CS cells (p<0.001). Neither recurrences nor metastasis were seen in the low grade group. 5 patients suffered a local recurrence and 2 had remote metastases in the high grade group. The CXCR4 expression levels increased in the recurrence/metastases samples for the 2 patients with more than one sample, indicating with progression of the tumor, the expression level of CXCR4 rises.

Conclusions: CXCR4 expression exists in all CS cells with its quantity and intensity increasing with progression which, in turn correlates with a poorer prognosis as assessed by recurrence or metastases.

37 Chemo-Resistant Ewing Sarcoma Is Susceptible to Natural Killer Cell-Mediated Cytotoxicity: Implications for Immunotherapy

D Berghuis, DHJ Verhoeven, SJ Santos, EP Buddingh, KL Schaefer, K Scottlandi, RM Egeler, MW Schilham, PCW Hogendoorn, AC Lankester. Leiden University Medical Center, Leiden, Netherlands; Heinrich-Heine University, Düsseldorf, Germany; Rizzoli Orthopaedic Institute, Bologna, Italy.

Background: Despite multimodal therapy, patients with refractory or relapsed Ewing sarcoma (EWS) have poor prognoses. To explore the feasibility of natural killer (NK) cell-mediated immunotherapy for patients with advanced-stage EWS, we investigated whether susceptibility of EWS to NK cell-mediated cytotoxicity is affected by chemo-sensitivity and identified pivotal molecular mechanisms involved in NK cell-mediated cytotoxicity.

Design: Expression of ligands for inhibitory and activating NK cell receptors was evaluated in chemo-resistant and -sensitive EWS cell lines (n=10) by flow cytometry. Cytotoxicity was determined in chromium release assays, using freshly isolated (resting) and interleukin (IL)-15 activated NK cells obtained from healthy donors. Blocking antibodies against specific ligands/receptors were used to study contribution of these molecules.

Results: All EWS cell lines were lysed by resting NK cells, regardless of chemo-sensitivity, except for one chemo-resistant cell line (CADO-ES). Ligands for the activating NK cell receptors DNAM-1 and NKG2D were expressed by all cell lines, though in heterogeneous patterns. Cytotoxicity depended on these receptors, since blocking either of these receptors abrogated cytotoxicity by resting NK cells. IL-15 activation of NK cells increased efficacy of lysis in all cell lines, including CADO-ES, and resulted in more efficient recognition of EWS cells, since only combined DNAM-1/NKG2D-blockade inhibited lysis. CADO-ES, resistant to lysis by resting NK cells, is characterized by high levels of HLA class I expression compared to other EWS cell lines; in addition, the HLA class I alleles expressed by CADO-ES are ligands for all inhibitory NK cell receptors (KIR). In this cell line, cytotoxicity by resting NK cells depended on loss of inhibition, since blocking antibodies against HLA class I reversed resistance. Induction or blockade of HLA class I did not significantly affect lysis in all other cell lines.

Conclusions: The observed susceptibility of chemo-resistant Ewing sarcoma to cytotoxicity by cytokine-activated NK cells may provide patients with advanced-stage Ewing sarcoma with an additional treatment modality.

38 Clusterin, a Follicular Dendritic Cell-Associated Apolipoprotein, Is Expressed in Normal Synoviocytes and in Tenosynovial Giant Cell Tumors of Localized and Diffuse Types: Diagnostic and Histogenetic Implications

JM Boland, AL Folpe, JL Hornick, KL Grogg. Mayo Clinic, Rochester, MN; Brigham and Women's Hospital, Boston, MA.

Background: Tenosynovial giant cell tumors (TGCT) comprise a family of lesions arising from synovium of joints, bursae or tendon sheath. TGCT are classified into localized (LTGCT) and diffuse (DTGCT) types, based on growth pattern and clinical behavior. TGCT were once thought to be reactive lesions, based on the heterogeneous histology including mononuclear cells, multinucleated giant cells, foam cells, and inflammatory cells. However, recent studies have shown recurrent clonal genetic abnormalities, confirming their neoplastic nature. The mononuclear component includes two cell types: small histiocytoid cells and large mononuclear cells (LMC) with abundant cytoplasm. The LMCs are positive for desmin in about 50% of cases, which highlights dendritic processes. The exact function and histogenesis of these cells has been unclear. The current study seeks to further characterize the phenotype of the cells comprising TGCT, and investigates the diagnostic utility of the marker clusterin, a recently identified follicular dendritic cell (FDC) associated glycoprotein that has diverse functions as a chaperone, lipoprotein transport, and cytoprotective protein.

Design: Immunostaining for clusterin was performed on 11 cases of LTGCT and 29 cases of DTGCT (23 intraarticular, 6 extraarticular). Most were also stained for desmin, the histiocyte marker CD163, and FDC markers CD21 and CD35.

Results: Clusterin staining was diffuse and strong in the LMCs in all cases. Desmin positivity was identified in 24/34 cases (71%), but was seen in only a subset of the LMCs (<5% to 80%), with 19/24 cases (79%) showing positivity in 10% or less of the LMCs. The LMCs were negative for CD163, CD21 and CD35. The smaller histiocytoid cells were positive for CD163, and negative for clusterin, CD21 and CD35. When present, adjacent non-neoplastic synovium was positive for clusterin and very focally positive for desmin.

Conclusions: Clusterin is a highly sensitive marker for TGCT, which has diagnostic utility in challenging cases, such as small biopsies, extraarticular DTGCT and cases with unusual histology. The observed staining patterns provide evidence linking the LMCs with normal synovial lining cells, and confirm that the LMCs are not of histiocytic derivation. Interestingly, clusterin expression and dendritic morphology are features shared by synovial lining cells and FDCs.

39 High Frequency of Chromosome 11 Loss in Embryonal Rhabdomyosarcoma Detected by SNP Array Tumoral Genotyping

D Bouron-Dal Soglio, AL Rougemont, R Absi, S Barrette, R Fetni, A Montpetit, JC Fournet. Hospital Sainte-Justine, Montreal, QC, Canada; Genome Quebec, Montreal, QC, Canada.

Background: Rhabdomyosarcoma (RMS) is the most frequent malignant pediatric soft tissue tumor. In pediatric population, RMS are divided into the more prevalent embryonal (ERMS) and the more aggressive alveolar rhabdomyosarcoma (ARMS), characterized by the presence of a translocation t(1;13)(p36;q14) or t(2;13)(q35;q14) in 80% of cases. In ERMS, no specific molecular abnormality has been yet described. However, 11p15.5 loss of heterozygosity (LOH) have been described in some ERMS, suggesting that a tumor suppressor gene in this region might be involved in the tumorigenesis of this model.

Design: We performed here the first whole-genome tumoral genotyping by high-definition SNP-array (Illumina Centrix 110 K) of a series of 11 pediatric RMS including 3 ARMS and 8 ERMS.

Results: A LOH at 11p15.5 has been observed in 7 out of 8 ERMS including 5 copy neutral LOH of the whole chromosome 11, a monosomy 11 and a copy neutral LOH limited to the 11p15.5 region. Numerical chromosomal abnormalities were also identified in ERMS, including trisomy 2, 7, 8 19 and 21. In contrast, a numerical chromosomal change was observed only in one ARMS. ARMS exhibited several different regional amplifications including amplification of the oncogenic fusion gene.

Conclusions: The high frequency of LOH at chromosome 11 or 11p15.5 in ERMS (7 out of 8) suggests us that they must be specific to ERMS comparing to ARMS and could be useful for the differential diagnosis of these two tumoral entities. They are underestimated in literature, regarding the lack of identification of copy neutral LOH by CGH array techniques.

40 Connexin 43 May Be a Potential Prognostic Biomarker for Ewing Sarcoma (EWS)/PNET

MM Bui, TL Pasha, G Acs, PJ Zhang. Moffitt Cancer Center, Tampa, FL; Hospital of the University of Pennsylvania, Philadelphia, PA.

Background: Connexin (Cx) is a family of homologous proteins that are building blocks of gap junctions (GJ) that permit direct exchange of small molecules between cells. Cx is vital in regulating cell proliferation and apoptosis, and is tumor suppressor in some and oncoprotein in other for carcinomas. Little is known for their role in sarcoma. We investigated the expression of Cx43 and Cx26 in EWS/PNET and correlated with various clinicopathologic data to explore its role in the biology of this group of tumor.

Design: Tissue microarray (TMA) consisted of 36 EWS/PNET patients (pts) from 1995-2007 were evaluated with clinicopathological data including tumor location, size, surgical margins, stage, treatment and survival. 4-µm TMA slides were immunohistochemically stained for Cx43 (CXN-6, 1:250, Santa Cruz) and Cx26 (rabbit polyclonal, 1:100, Zymed). Immunoreactivity was quantitatively evaluated by automated slide scanning using Aperio ScanScope XT (Vista, CA) and Image Pro Plus v6.2 (Bethesda, MD) analysing macro algorithms based on the intensity (0-3) and % of staining. A score of 0-300 is calculated for each case as the product of the intensity score and the %. The level of expression was analyzed with various clinicopathologic factors.

Results: Among 36 pts, 19 were alive and 17 dead (median follow up 410 days). Cytoplasmic Cx43 reactivity was detected in 28/36 (78%) cases (score ranged 1-160, median 62). The score of Cx43 reactivity significantly differed between tumors from alive (median 50) and dead (median 105) pts ($p=0.0036$, Mann-Whitney). When tumors were divided by median into high and low Cx43 groups, 13/18 (72%) low Cx43 tumors were from alive pts while 12/18 (67%) high Cx43 tumors from deceased ($p=0.04$, Fisher's exact test). The survival difference in low and high Cx43 groups approached significance (median survival 2,388 vs. 701 days, $p=0.0552$, Log-Rank). Cytoplasmic Cx26 reactivity was detected in 2 of 36 (6%) cases. In both cases, the patients died with metastasis (lung and brain) in 341 days and 211 days, respectively.

Conclusions: EWS/PNET express cytoplasmic Cx43 frequently (78%) and Cx26 rarely (6%). The level of Cx43 expression correlated with outcome of EWS/PNET, regardless of their stage, location, size and management. Study in a larger series is warranted to confirm its prognostic role. Our results also suggest a possible oncogenic role of Cx 43 and less likely Cx 26 in EWS/PNET. The lack of membrane reactivity suggests that these Cx likely function in a GJ independent mechanism.

41 Epithelioid Sarcoma Expresses Epidermal Growth Factor Receptor but Gene Amplification and Kinase Domain Mutations Are Rare

MJ Cascio, RJ O'Donnell, AE Horvai. UCSF, San Francisco, CA.

Background: Epithelioid sarcoma is a rare, malignant, soft tissue neoplasm that can be classified into proximal, distal and fibroma-like subtypes. Regardless of subtype, epithelioid sarcoma often demonstrates morphologic and immunophenotypic evidence of epithelial differentiation. Current therapeutic strategies include radical resection, amputation, radiation or chemotherapy although prognosis is poor. Epidermal growth factor receptor (EGFR) is a novel therapeutic target in carcinomas. In some carcinomas, EGFR kinase domain mutations or gene amplification may correlate with response to specific inhibitors. EGFR expression has been reported in some sarcomas, but expression, amplification and kinase mutations have not been studied in epithelioid sarcoma.

Design: We evaluated 13 cases of epithelioid sarcoma (6 distal, 6 proximal and 1 fibroma-like) for expression of EGFR by immunohistochemistry using formalin-fixed, paraffin-embedded tissue. Each sample was stained and scored according to established methods (EGFR pharmDx, Dako, Carpinteria, CA) and the fraction of cells staining was also recorded. EGFR gene amplification and polysomy were evaluated using fluorescence in situ hybridization (FISH) performed on paraffin-embedded tissue. All cases were tested for kinase domain mutations (exons 18-21) by PCR and direct sequencing.

Results: Twelve of thirteen epithelioid sarcomas (92%) showed expression of EGFR by immunohistochemistry. Most cases ($n=8$, 62%) showed strong (3+) and homogeneous (>75% of cells) membrane staining. FISH demonstrated no amplification of the EGFR gene (EGFR:centromere ratios ranged from 0.93 to 1.03). Forward and reverse nucleotide sequencing of the tyrosine kinase domain of the EGFR gene (exons 18-21) failed to reveal point mutations, insertions, or deletions in any case.

Conclusions: EGFR is expressed in most epithelioid sarcoma regardless of subtype. However, EGFR gene amplification and activating mutations in the tyrosine kinase domain appear to be rare or absent in these tumors. Thus, the benefit of targeted therapy against EGFR in patients with epithelioid sarcoma remains to be determined.

42 The Sonic Hedgehog Pathway in Chordoma

JM Cates, DM Itani, KC Homlar, SJ Olson, GE Holt, HS Schwartz, CM Coffin, BD Harfe. Vanderbilt University Medical Center, Nashville, TN; Vanderbilt Orthopaedic Institute, Nashville, TN; University of Florida, Gainesville, FL.

Background: Chordomas are malignant primary bone tumors that show morphologic and molecular evidence of notochordal differentiation. Sonic hedgehog (SHH) is a crucial morphogen secreted by the fetal notochord that directs embryonic patterning of the neural tube and adjacent sclerotomes. In contrast to the early fetal notochord, putative intraosseous notochordal remnants recently identified in mice do not appear to express SHH. It is unknown whether the nucleus pulposus of the adult intervertebral disc (IVD), benign notochordal cell tumors (BNCT), or chordomas express SHH or the SHH receptor/signaling complex, patched (PTCH) and smoothened (SMO). However, genetic studies have documented gains of chromosome 7q36, which contains the SHH locus, in many chordomas.

Design: Archived chordal tissue samples were stained for SHH and PTCH by immunohistochemistry. Skull base chondrosarcomas were stained for comparison. SHH was considered positive if >10% cells showed cytoplasmic staining of at least moderate intensity. For PTCH, the presence of any specific cytoplasmic immunoreactivity was considered positive.

Results: SHH is expressed in human fetal notochord and chordomas of the sacrum ($n=11$), skull base ($n=12$), and mobile spine ($n=4$). In contrast to fetal notochord, PTCH is co-expressed in 92% of SHH-positive chordoma samples. Notably, the 2 BNCTs examined are negative for SHH and PTCH, as are most chondrosarcomas, IVDs, and the 1 dedifferentiated chordoma studied.

SHH and PTCH Expression in Chordal Tissues and Skull Base Chondrosarcoma

	n	SHH+	PTCH+
Conventional chordoma	23	22	20
Chondroid chordoma	4	4	4
Dedifferentiated chordoma	1	0	0
Benign notochordal cell tumor	2	0	0
Chondrosarcoma	6	1	1
Nucleus pulposus of IVD	7	1	0/3
Notochord	2	2	0

Conclusions: SHH and its cognate receptor PTCH are co-expressed in most chordomas. In contrast, this pathway does not appear active in human notochord (at the gestational ages examined), nucleus pulposus of the adult IVD, or in BNCT. SHH signaling is not activated in chondrosarcoma or in chordomas that have undergone dedifferentiation.

Whether aberrant activation of this autocrine signaling pathway contributes to chordomagenesis should be investigated further in murine models and in putative precursor lesions of chordoma such as BNCT and notochordal rests.

43 FNCLCC Grading for Core Needle Biopsies of Soft Tissue Sarcomas Using Ki-67 Proliferative Activity and Radiologic Assessment of Necrosis

S Davion, X Lin, I Omar, W Laskin. Northwestern Memorial Hospital, Chicago, IL.

Background: Optimal patient management for high grade soft tissue sarcomas (STS) may involve *preoperative* chemoradiation therapy. Core needle biopsies (CNB) are preferred for initial diagnosis of STS because of their efficiency and lack of morbidity, but grading such small samples proves difficult. FNCLCC combines mitotic index, % necrosis, and differentiation, for a three-tiered grading system and is used on surgical resection specimens. However it is poorly transferrable to the limited tissue of CNB.

Design: In this study, we correlated FNCLCC grade on CNB with final surgical excision FNCLCC grade for 17 biopsied and resected STS. For CNB we used Ki-67 immunoreactivity instead of mitotic count and evaluated the amount of necrosis radiographically.

Results: The CNB FNCLCC grade accurately predicted the surgical specimen FNCLCC grade in 10 out of 16 cases ($r = .60$, $p = .005$). FNCLCC grade between surgical excision and CNB never differed by more than one. Radiologic assessment of necrosis accurately predicted surgical specimen necrosis in 10/12 malignant cases (100% sensitive, 75% specific), and 2 out of 7 benign soft tissue tumors used as controls (28% specific). The FNCLCC CNB differentiation grade accurately predicted the surgical excision differentiation grade in 11 out of 16 ($r = .38$, $p = 0.14$) cases. Most discrepancies in differentiation grade occurred in the well differentiated liposarcoma group where more cellular/differentiated areas, or areas not diagnostic of liposarcoma, were not sampled on the CNB. The Ki-67 index accurately predicted the surgical specimen FNCLCC mitotic grade in 8 of 13 cases ($r = .48$, $p = .09$). All CNBs with a Ki-67 index of less than 13% had a surgical mitotic FNCLCC grade of 1. The Ki-67 index of all 7 benign soft tissue lesions used as controls was less than or equal to 1%.

Conclusions: FNCLCC grading of CNB using radiologic assessment of necrosis and Ki-67 index to supplant mitotic activity shows a moderate degree of correlation with the surgical resection specimen grade using conventional FNCLCC criteria. CNB assessment of differentiation is least reliable in the well-differentiated liposarcoma group. Absence of radiologic necrosis in a malignant STS virtually assured its absence in the surgical resection specimen.

44 Clinicopathologic Analysis of Adult Alveolar and Embryonal Rhabdomyosarcoma: A Study of 62 Cases

AT Deyrup, K Thway, C Fisher, W-L Wang, AJ Lazar, RL Jones, M Tighiouart, SW Weiss. Emory University, Atlanta; Royal Marsden, London, United Kingdom; MD Anderson, Houston.

Background: Embryonal (ERMS) and alveolar (ARMS) rhabdomyosarcoma are rare in adults and are not well characterized in this patient population: we report 62 cases of ERMS and ARMS arising in patients 40 years and older.

Design: Sixty-two patients who were 40 years or older with RMS were identified from surgical pathology and consultation files, excluding pleomorphic RMS. Clinicopathologic information included tumor site, patient age, detailed treatment information and translocational analysis.

Results: Sixty-two adult patients (age 40-82 yrs; mean 56 yrs; 35M:27F) with RMS from 1 to 40 cm (mean 10.2 cm) were identified. Tumors arose in the head/neck (n=19), thorax (n=15), extremities (n=13), abdomen/pelvis (n=9) and genitourinary system (n=6) and were classified as Intergroup RMS Pretreatment staging system I(10), 2(3), 3(26) and 4(19). Microscopically, 29 cases were classified as ERMS and 14 as ARMS. Mitotic activity ranged from 0-126 mit/10 hpf (mean 34); 37 cases showed at least focal necrosis. By immunohistochemistry, 47/47 tumors expressed desmin, 41/41 expressed myogenin and 18/18 expressed MyoD1. 26 cases were translocation-negative; 4 cases had t(2;13) and 1 had t(1;13). 4 cases with alveolar histology were translocation-negative. No ERMS was translocation-positive. Follow-up information was available in all cases: 40 patients died of disease (0-78 mos, mean 18.2 mos). 5-year disease-specific survival was 24.4%; of the 22 patients who did not die of disease, survival ranged from 0 to 168 mos (mean 55 mos). 34 patients had metastatic disease (lung, 18; lymph node, 17; soft tissue, 10; bone, 8; liver, 4; other, 9). 40 patients were treated with chemotherapy and 30 patients received radiation. By univariate analysis, IRS stage ($P=0.001$), size ($P=0.007$), metastasis ($P=0.02$) and location in abdomen/pelvis or thorax compared to extremity ($P=0.03$) were significant indicators of death from disease. Patient age ($P=0.88$), sex ($P=0.13$), alveolar histology ($P=0.77$) and treatment with chemotherapy ($P=0.15$) did not affect disease-specific survival.

Conclusions: ARMS and ERMS arising in adults differ from those in children: 1) alveolar histology is not associated with an increased risk of death; 2) chemotherapy does not significantly affect disease-specific survival; and 3) adults present with advanced stage disease and have a worse prognosis.

45 Evaluation of TFE3 Expression in Tumors of Microphthalmia-Associated Transcription Factor (MiTF) Family and Its Potential Diagnostic Significance

BC Dickson, JS Brooks, TL Pasha, PJ Zhang. Pennsylvania Hospital, Philadelphia; Hospital of University of Pennsylvania, Philadelphia.

Background: TFE3 is a DNA-binding factor closely related to microphthalmia-associated transcription factor (MiTF). Immunohistochemistry for TFE3 is routinely used to detect the gene fusion product in alveolar soft part sarcoma (ASPS) and Xp11-translocation renal cell carcinomas. Recently, TFE3 expression has been identified in PEComas, implying a possible role of TFE3 in the MiTF family of tumors. Our study

examined TFE3 expression amongst other members of the putative MiTF group of neoplasms.

Design: Fifty-one tumors of the MiTF family were available for study. These included cases of PEComa (PEC, N3), angiomyolipoma (AML, N22), metastatic malignant melanoma (MMM, N16) and clear cell sarcoma (CCS, N9). Two cases of ASPS were included for comparison. All cases were re-reviewed to verify the diagnosis. Immunohistochemistry was performed on formalin-fixed paraffin-embedded sections with goat anti-human TFE3 (1:600; sc-5958; Santa Cruz Biotechnology, CA) with heat-induced antigen retrieval in Citrate Buffer. IHC detection was performed on a DAKO Autostainer. Nuclear staining was semiquantified using the Allred scoring method, which assesses both the intensity (0-to-3) and percentage (0-to-5) of positive nuclei; cases with a combined score of ≤ 3 were arbitrarily defined as negative.

Results: Seventy-five percent of cases (38/51) tested positively, as follows: 3/4 PEC (average Allred score = 5.2), 18/22 AML (average Allred score = 4.6), 11/16 MMM (average Allred score = 4.3) and 6/9 CCS (average Allred score = 4.3). Compared to the cases of ASPS (average Allred score = 8.0), TFE3 staining was less intense and had greater variability in overall expression in the MiTF family of tumors.

Conclusions: Nuclear TFE3 can be detected in approximately 75% of the MiTF group of tumors. In addition to PEC, our data demonstrate for the first time that expression of TFE3 protein is common to all known members of the MiTF family of neoplasms including AML, CCS and MMM. While TFE3 expression tended to be variable and less intense than in ASPS, our results indicate that tumors of the MiTF family should be considered in the differential diagnosis when nuclear TFE3 reactivity is detected, particularly when the reactivity is focal and weak, and differentiated from ASPS and Xp11-translocation renal cell carcinomas.

46 CNS and MSK Mesenchymal Chondrosarcoma: A Malignant Cartilage Tumor with Metaplastic Hyaline Cartilage that Recapitulates Growth Plate Endochondral Ossification

JC Fanburg-Smith, A Auerbach, JS Marwaha, Z Wang, EJ Rushing. Armed Forces Institute of Pathology, Washington, DC.

Background: Mesenchymal chondrosarcoma (MCHSA), a rare malignant biphasic round cell and hyaline cartilage tumor, is most commonly musculoskeletal (MSK), but can occur in central nervous system (CNS). Sox9, a master regulator of chondrogenesis, was previously demonstrated by IHC in intraosseous MCHSA and conventional CHSA. Nuclear beta-catenin, involved in the Wnt/APC pathway, has been observed by IHC in CHSA, but not MCHSA. Osteocalcin (OC), a non-collagenous bone protein, was identified by IHC in osteosarcoma cells and matrix.

Design: Morphology and IHC and follow-up on MSK and CNS MCHSA and control cases from our files were obtained and studied.

Results: 22 MCHSA included 5 CNS (all female, mean age 30.2, mean size 7.8 cm, in frontal lobe (n=4) and spinal cord (n=1)) and 17 MSK (11F:6M, mean age 31.1, mean size 6.2 cm, 3 each of humerus and vertebrae, 2 each of pelvis, rib, tibia, neck soft tissue, one each of femur, unspecified bone, elbow soft tissue). CNS and MSK MCHSA had similar round cells, staghorn vasculature, increased mitotic activity, and centrally located metaplastic cartilage islands, in a zonal pattern from immature to proliferating to hypertrophic chondrocytes, then exhibiting cell death; 67% had central endochondral ossification (cells and matrix positive for OC). SOX9 reacted in 21/22 (95%) MCHSA in round cells and cartilage island chondrocytes. Beta-catenin highlighted cells adjacent to cartilage matrix in 35%. Round cells were 100% INI positive and 50% focal desmin and rare S100 and EMA positive, but negative for MyoD1, keratins, SMA, lymphoid markers, CD34, CD99, GFAP, ER, PR, and OC. Control small cell OSA were positive for OC, negative for SOX9. 80% patients with follow-up had pulmonary metastases and/or died within a mean of 5 years.

Conclusions: CNS and MSK MCHSA predominantly affect adult females with poor prognosis. Centrally, MCHSA forms hyaline cartilage that undergoes endochondral ossification, a metaplastic recapitulation of growth plate cartilage. Sox9 positivity supports cartilage phenotype. OC demonstrates bone cells and matrix resulting from endochondral ossification in central cartilage islands and is negative in round tumor cells, separating MCHSA from small cell osteosarcoma. Focal nuclear beta-catenin adjacent to cartilage supports the role of beta-catenin in chondrogenesis in MCHSA. SOX9 and OC and morphologic detail can separate MCHSA from other MSK and CNS round cell tumors.

47 A Study of MITF/TFE Transcription Factors and Melanocytic Differentiation Markers in Angiomyolipomas

F Francis, D Nonaka. New York University School of Medicine, New York, NY.

Background: Angiomyolipomas (AMLs) belong to a family of so-called perivascular epithelioid cell tumors (PEComas) that share muscular and melanocytic differentiation. Despite extensive investigation, the histogenesis and lineage of AMLs remain unclear. It has been reported that AMLs express melanocytic-associated antigens such as HMB-45 and Melan A to a greater extent than MITF and tyrosinase family of proteins for yet unknown reasons. A normal cell counterpart has not been found; however, owing to its melanocytic differentiation, AMLs have been suggested to be of neuroectodermal origin. In this study, we investigated the expression of the MiT (MITF/TFE) family of transcription factors and melanocytic differentiation markers in AMLs in order to comprehend the mechanisms of melanocytic differentiation.

Design: Twenty AMLs of renal and peri-renal regions were retrieved from the NYU Medical Center database, and immunohistochemistry studies were performed for Sox10 (neuroectodermal stem cell marker), MITF, TFE3, TFEB, TFEC, Tyrosinase, TRP1, TRP2, HMB-45 and Melan A. The extent of staining was graded as 1+ (1-25% of cells positive), 2+ (26-50%), 3+ (51-75%) and 4+ (76-100%).

Results: Sox10 was completely negative in all AMLs. MITF was expressed in 42% of the tumors with focal (1+ and 2+) reaction except for one tumor with 3+ expression. In contrast, TFE3 expression was diffuse (3+ and 4+) in all tumors. TFEB and TFEC

were completely negative. HMB-45 and Melan A were expressed in all cases, and their reactions were diffuse in 42% and 26% of the tumors, respectively. Tyrosinase expression was only focal in all AMLs except for one tumor with a 3+ expression. TRP1 was variably expressed with 32% of the cases showing diffuse reaction, and TRP2 expression was focal in all tumors except for two negative cases.

Conclusions: A completely negative reaction to Sox10 in all AMLs indicates that they are probably of mesenchymal origin rather than of neural crest derivation. AMLs show full blown melanocytic differentiation, as evidenced by expression of all the melanocytic-specific markers and tyrosinase-related proteins. Diffuse expression of TFE3 in all AMLs in comparison to focal MITF reaction in 42% of the tumors suggests that TFE3, probably in conjunction with MITF, plays a major role in the melanocytic differentiation in AMLs.

48 EGFR Expression, Amplification and Kinase Domain Mutations Are Rare in Epithelioid Vascular Neoplasms

R Gill, RJ O'Donnell, AE Horvai. UCSF, San Francisco, CA.

Background: Epithelioid vascular neoplasms represent a spectrum of tumors ranging from benign epithelioid hemangioma, intermediate grade epithelioid hemangioendothelioma to malignant epithelioid angiosarcoma. Patients diagnosed with the latter two uncommon tumors have few therapeutic options and might benefit from targeted inhibition of epidermal growth factor receptor (EGFR) tyrosine kinase activity. Treatment with kinase inhibitors has been well established for carcinomas, in which the presence of kinase domain mutations or EGFR gene amplification may correlate with clinical response to specific inhibitors.

Design: We evaluated 17 epithelioid hemangioendotheliomas (EHE) and 10 epithelioid angiosarcomas (EA) for EGFR expression by immunohistochemistry, on formalin-fixed paraffin embedded tissue. Each sample was scored (1-4+) and characterized as positive or negative. Positive cases were further analyzed by dual color fluorescence in-situ hybridization (FISH) for EGFR amplification or polysomy. Finally, positive cases were tested for kinase domain mutations in exons 18-21 by PCR and direct sequencing.

Results: Three of the EHE cases (18%) and one EA case (10%) had detectable membrane EGFR by immunohistochemistry with 1+ to 3+ intensity and 25% to 100% of tumor cells staining. However, none of these demonstrated EGFR gene amplification by FISH (EGFR to centromere ratios ranged from 0.85 to 1.0). One EHE case demonstrated a single base change in exon 19. This corresponded to a P753R missense mutation. A second EHE case demonstrated a silent base change in exon 20 (at Gln⁷⁸⁷). None of the EA cases demonstrated mutations in exons 18-21 of EGFR.

Conclusions: The expression of EGFR is rare in EHE and EA. A subset of these epithelioid vascular tumors demonstrate immunohistochemically detectable EGFR but the absence of gene amplification and rarity of kinase domain mutations suggests that few patients, if any, may benefit from targeted therapy.

49 Distinct MicroRNA Expression Profiles in Synovial Sarcoma and Ewing Family of Tumors

M Hisaoka, A Matsuyama, H Hashimoto. School of Medicine, University of Occupational and Environmental Health, Kitakyushu, Japan.

Background: MicroRNAs (miRNAs) are processed, short non-coding RNAs that can influence a variety of biological processes such as development, proliferation and differentiation. Recently, miRNA expression patterns have been suggested to be closely related to phenotypes and biological behaviors of some epithelial, hematological and mesenchymal malignancies including limited types of soft tissue sarcomas. It is unknown whether miRNA status is also distinct between fusion-associated soft tissue sarcomas with potential overlapping phenotypes such as synovial sarcoma and the Ewing family of tumors.

Design: We performed a comparative analysis of miRNA expression profiles of 15 synovial sarcomas and 5 Ewing sarcomas/primitive neuroectodermal tumors with known tumor-type specific gene fusions using RNA extracted from their frozen tissues and 3D-Gene miRNA microarrays, carrying more than 700 miRNA probes (Toray, Kamakura, Japan). Non-neoplastic adult skeletal muscle tissues (n=5) were used as normal controls.

Results: Unsupervised hierarchical clustering analysis demonstrated unique miRNA expression signatures of both tumor types and control tissues. Using ANOVA and Tukey's multiple comparison, six miRNAs, including let-7e and miR-134, were identified to discriminate each group from others ($p < 0.038$).

Conclusions: Despite the potential overlapping morphologic and immunophenotypic features, synovial sarcoma and the Ewing family of tumors show distinct miRNA profiles. Our data suggests a possible diagnostic role of the miRNA profiling and warrants further investigations of miRNA-dependent molecular mechanisms of the development of these mesenchymal tumors.

50 Hybrid Schwannoma/Perineurioma: Analysis of 39 Distinctive Benign Nerve Sheath Tumors

JL Hornick, EA Bundock, CDM Fletcher. Brigham & Women's Hospital, Harvard Medical School, Boston, MA.

Background: Several years ago, our group presented a small series of benign nerve sheath tumors showing hybrid features of schwannoma and soft tissue perineurioma. The purpose of this study was to further characterize a large series of these lesions.

Design: 39 cases received between 1994 and 2008 were retrieved from authors' consult and surgical pathology files. Clinical details and follow-up were obtained from referring pathologists. H&E sections were re-examined, and immunohistochemistry was performed. On 10 cases, double staining with EMA (HRP) and S100 (Alk Phos) was performed.

Results: 21 patients were female, and 18 male (mean age 38 years; range 2-85; 70% 2nd-5th decades). Most patients presented with a painless nodule. The tumors arose in a

wide distribution: 16 lower limb; 12 upper limb; 6 head & neck; 4 trunk; 1 colon. None of the patients showed signs of neurofibromatosis (NF). Tumor size ranged from 0.7-17.5 cm (mean 3 cm). Most tumors involved superficial subcutis (8 also dermis); only 2 were intramuscular. Histologically, the tumors were usually well-circumscribed but unencapsulated, and composed of spindle cells with plump, tapering nuclei and pale eosinophilic cytoplasm with indistinct cell borders, arranged in a storiform, whorled, and/or lamellar architecture. Only one tumor showed infiltrative margins. One tumor showed a plexiform growth pattern. Antoni A and B zonation and hyaline vessels were absent. Six tumors showed focally myxoid stroma, and 10 showed scattered cells with degenerative nuclear atypia. Mitoses ranged from 0-4 per 30 HPF; 29 had no mitoses. All tumors showed staining for S100 and EMA; 97% were positive for CD34, 85% for GFAP, and 78% for claudin-1. Twelve tumors contained rare NFP-positive axons. Double staining for EMA and S100 revealed parallel layers of alternating S100 and EMA-positive cells with no co-expression of antigens by the same cells. Most tumors were composed of 60-70% Schwann cells and 30-40% perineurial cells. After a mean follow-up of 24 months (range: 6-60 months), 1 tumor recurred locally, following incomplete excision.

Conclusions: Benign nerve sheath tumors showing predominantly schwannian cytomorphology and perineurioma-like architecture are composed of an admixture of both cell types. These tumors usually arise in the dermis and subcutis and occur over a wide age range and anatomic distribution. Degenerative nuclear atypia (akin to ancient schwannoma and atypical neurofibroma) is relatively common. Hybrid schwannoma/perineuriomas have no association with NF and rarely recur.

51 Heterogeneity of Genetic Alterations in Dedifferentiated Liposarcoma

AE Horvai, S DeVries, R Roy, RJ O'Donnell, F Waldman. UCSF, San Francisco, CA.

Background: Liposarcoma is the most common soft tissue sarcoma in adults. Progression from well-differentiated liposarcoma to a dedifferentiated form is a rare, but well documented, phenomenon. Amplification of chromosome subregion 12q13-q15 is present in both well- and dedifferentiated liposarcomas and the resulting amplifications of cell cycle regulators MDM2 and CDK4 may promote tumorigenesis. However, the genetic changes that distinguish between well- and dedifferentiated liposarcomas, and may provide insight into progression, are less well understood. The relationships between genetic changes and either clinical presentation or tumor grade are also unknown.

Design: We used array comparative genomic hybridization to study the genetic changes in 29 cases of dedifferentiated liposarcoma. Well-differentiated and dedifferentiated components were microdissected and separately analyzed, allowing pairwise comparisons of genetic data and differentiation. Genetic changes were also compared to clinical presentation, grade and expression of MDM2 and CDK4.

Results: All 29 cases showed amplification of 12q13-15. Using unsupervised hierarchical clustering, the tumors could be resolved into three categories based on the severity of genomic aberrations. The paired well-differentiated and dedifferentiated components differed with respect to the total number of amplifications ($p = 0.008$). High level amplifications of 1q23-24 and 6q21-23 were present in 5 cases each (17%) but no genetic changes were statistically significant in separating well-differentiated and dedifferentiated components. In four cases (14%), a well-differentiated liposarcoma preceded the dedifferentiated liposarcoma by 1-5 years ("secondary"). Eight cases (28%) were classified as low-grade dedifferentiation. Interestingly, secondary presentation and grade correlated with the frequency of genetic changes at 4 and 6 specific loci, respectively ($p = 0.01$). Secondary tumors also showed more total genomic variability than primary tumors ($p = 0.026$). CDK4 and MDM2 immunopositivity demonstrated a synergistic effect on amplification at 12q13-15.

Conclusions: Dedifferentiated liposarcomas are genetically heterogeneous tumors with reproducible changes, but none that uniformly distinguish the well- and dedifferentiated components. The relationship between presentation, grade and genetic changes may reflect differences in tumor initiation, factors that control genomic instability or the background genotype of the tumor.

52 MGC3032-MKL2 Is the Resulting Fusion Oncogene of t(11;16)(q13;p13) in Chondroid Lipoma

D Huang, J Sumegi, JD Reith, P Dal Cin, T Yasuda, M Nelson, JA Bridge. University of Nebraska Medical Center, Omaha, NE; Cincinnati Children's Hospital Medical Center, Cincinnati, OH; University of Florida College of Medicine, Gainesville, FL; Brigham and Women's Hospital, Boston, MA.

Background: Chondroid lipoma (ChL), a rare benign adipose tissue tumor, may histologically resemble myxoid liposarcoma or myxoid chondrosarcoma. In the current study, cytogenetic analysis of 3 ChLs revealed a t(11;16)(q13;p13) in all 3 cases, a finding consistent with previous isolated reports. We hypothesized that this primary translocation generates a fusion gene of central pathogenic relevance in ChL. Our study objectives were to: 1) further localize the t(11;16) chromosomal breakpoints in ChL; 2) uncover the underlying involved genes; and, 3) establish new molecular diagnostic assays for ChL.

Design: A fluorescence in situ hybridization (FISH)-based positional cloning strategy using a series of bacterial artificial chromosome (BAC) probe combinations on ChL abnormal metaphase cells was employed for narrowing the t(11;16) breakpoints. Following identification of *MKL2* as the candidate gene on 16p13, *MKL2* gene specific primers were designed and 5' RACE studies conducted. Subsequently, all 3 ChLs were subjected to RT-PCR analysis using fusion transcript specific primers followed by sequencing. Lastly, interphase FISH studies were also performed on all 3 cases utilizing newly established dual fusion probe sets.

Results: Metaphase FISH analysis revealed single BAC probes covering the chromosome 11 and 16 breakpoint regions; the latter corresponding to the *MKL2* gene locus. 5' RACE identified *MGC3032* as the *MKL2* partner gene and sequencing studies of the RT-PCR generated transcripts defined the fusion occurring between exons 5 and

9 of *MGC3032* and *MKL2* respectively. Identical fusion transcripts were confirmed in all 3 ChL cases. Interphase FISH studies showed the anticipated rearrangements of the *MGC3032* and *MKL2* loci.

Conclusions: ChL is characterized by chromosomal translocation t(11;16)(q13.1;p13) resulting in the fusion of the *MGC3032* and *MKL2* genes. Megakaryoblastic leukemia 2 (*MKL2*) encodes for myocardin-related transcription factor B (MRTF-B) in a megakaryoblastic leukemia gene family, and *MGC3032* is a hypothetical protein. Additional studies must be conducted to determine the functionality of this unique *MGC3032-MKL2* fusion oncogene in ChL. Novel FISH and RT-PCR assays developed in this study can serve as diagnostic adjuncts for this rare entity.

53 Clinical Aggressiveness of Myxofibrosarcomas Is Associated with Decreased Expression of p12^{CDK2AP1}: Prognostic Implication of a Putative Tumor Suppressor That Induces Cell Cycle Arrest and Apoptosis Via Mitochondrial Pathway

HY Huang, YL Chen, CF Li, YL Shiu. Chang Gung Memorial Hospital, Kaohsiung Medical Center, Chang Gung University, Kaohsiung, Taiwan; National Sun Yat-Sen University, Kaohsiung, Taiwan; Chi-Mei Foundation Medical Center, Tainan, Taiwan.

Background: The tumorigenesis and prognostication of myxofibrosarcoma remains obscure. Attenuated endogenous expression of P12^{CDK2AP1} and its active dimmer (P25^{CDK2AP1}) was found in myxofibrosarcoma cell lines (NMFH-1, OH931), prompting us to investigate the clinical and biological significance of this putative tumor suppressor that targets CDK2 for proteolysis.

Design: A polyclonal antibody against the P12^{CDK2AP1}-His fusion protein was generated to perform Western blotting and immunohistochemistry. Vectors of p12^{CDK2AP1}-specific cDNA and shRNA were transfected into NMFH-1 cells to analyze the effects on CDK2 expression, cell cycle regulation by flow cytometry, and apoptotic responses by assessing changes in annexin V and caspase-3, 8, 9. By tissue microarrays, P12^{CDK2AP1} immunostain was interpretable in 102 primary myxofibrosarcomas and correlated with clinicopathological variables, expression of CDK2 and cleaved caspase-3, and disease-specific survival (DSS).

Results: Exogenous P12^{CDK2AP1} overexpression in NMFH-1 cells induced cell cycle arrest at G0/G1 phase and downregulated CDK2 expression, and these findings were reversed by RNA interference. In NMFH-1 cells, increased cleaved products of caspases-3, 9, but not caspase-8, were detected after transfecting P12^{CDK2AP1}-specific cDNA, suggesting the induction of apoptosis via the mitochondrial pathway. P12^{CDK2AP1} immunostain, aberrantly decreased in 63% of cases, was positively and negatively related to the expression of cleaved caspase-3 ($p < 0.001$) and CDK2 ($p = 0.034$), respectively. Together with higher histological grades, decreased P12^{CDK2AP1} expression was predictive of worse DSS in both univariate ($p = 0.002$) and multivariate ($p = 0.015$) analyses.

Conclusions: P12^{CDK2AP1} expression induces both mitochondrial pathway-dependent apoptosis and cell cycle arrest with downregulated CDK2. Declined P12^{CDK2AP1} expression also represents a poor prognosticator of myxofibrosarcomas.

54 Protein Kinase C-theta Expression in Ewing Sarcoma/Primitive Neuroectodermal Tumor and Malignant Peripheral Nerve Sheath Tumor

GH Kang, KM Kim, DY Kang, CK Park. Samsung Medical Center, Seoul, Korea; Chungnam National University, Daejeon, Korea.

Background: Systemic treatment options for advanced sarcomas remain limited. No new effective drugs have been recently described and proposed for sarcomas and, therefore, innovative treatment modalities are very welcome and needed. Recently, it has been reported that protein kinase C (PKC)-theta can serve as a novel therapeutic target in gastrointestinal stromal tumor. PKC-theta is involved in neuronal differentiation and is expressed in the nervous system.

Design: To explore PKC-theta expression in Ewing sarcoma/primitive neuroectodermal tumor (ES/PNET) and malignant peripheral nerve sheath tumor (MPNST), 21 ES/PNETs and 19 MPNSTs having typical histopathologic and immunohistochemical findings were retrieved from surgical pathology files from Jan 2000 to July 2008. Formalin-fixed, paraffin-embedded tissue was used for PKC-theta immunostaining (clone 27, BD Transduction Laboratories, 1:100). The expression was considered as positive when at least 10% of the tumor cells were stained. The intensity was graded as negative, weak, moderate or strong.

Results: PKC-theta was positive in the cytoplasm of tumor cells. The staining pattern was predominantly diffuse, and dot-like staining was observed in 2 ES/PNET cases. Seven out of 21 (33.3%) cases of ES/PNETs and 17/19 (89.5%) MPNSTs were positive for PKC-theta. In ES/PNETs, the staining intensity was strong and moderate in 1 each case and weak in 5 cases. In MPNSTs, the staining intensity was strong in 4, moderate in 6, and weak in 7 cases.

Conclusions: We first identified PKC-theta expression in ES/PNETs and MPNSTs with a high frequency and strong intensity. Characteristic dot-like staining pattern observed in ES/PNET can also serve as a diagnostic utility. Although biological function of PKC-theta in ES/PNET and MPNST has yet to be explored, our novel findings highlight that PKC-theta warrants clinical evaluation as a potential therapeutic target in those highly aggressive soft tissue sarcomas.

55 An Audit of Lipomatous Neoplasms: Correlation with MDM2 Amplification by Fluorescence In Situ Hybridisation

TG Kashima, DD Halai, R Tirabosco, S Hing, H Ye, AM Flanagan. Royal National Orthopaedic Hospital NHS Trust, London, United Kingdom; UCL, London, United Kingdom; University of Cambridge, Cambridge, United Kingdom.

Background: MDM2 amplification has been reported as being a sensitive means of distinguishing lipomas from atypical lipomatous tumours/well differentiated liposarcomas (ALT/WDL). The aim of this study was to discover if employing MDM2

FISH for distinguishing between these 2 tumour types would be valuable in clinical practice.

Design: The microscopy of 139 benign/low grade and 25 high grade lipomatous neoplasms were reviewed by 3 pathologists (blinded to the clinical information) and the results correlated with the presence and absence of MDM2 amplification (MDM2 & CEP12 probes provided by Zytovision). 50 cells with at least two CEP12 signals were counted in each case. Cases were considered to be positive for MDM2 amplification if the MDM2:CEP12 ratio was equal to or more than 2.

Results: FISH was found to be informative in all cases. 59 of the 164 cases had MDM2 amplification. There was 100% agreement between the pathologists when making diagnoses of hibernoma (n=10), lipoblastoma (n=5), spindle cell lipoma (n=14) and pleomorphic liposarcoma (n=10); none of these tumours harboured MDM2 amplification. 13 of 15 cases of the dedifferentiated component of ALT/WDL revealed MDM2 amplification. Of the remaining 110 cases (conventional lipomas and ALT/WDL) 46 revealed an MDM2 amplification and 67% of these were unequivocally considered histologically to represent ALT/WDL by all pathologists. The tendency was to overcall these mature lipomatous tumours. The tumours that were undercalled contained only a few scattered atypical cells whereas the majority of the small tumour cells in these neoplasms revealed MDM2 amplification. The average size of tumours reassessed as lipoma or ALT/WDL on the basis of MDM2 amplification was 16.4 cm (range 4-31 cm) and 15.7 cm (3.5-29 cm) respectively ($p > 0.05$), indicating tumour size is unhelpful in distinguishing between these tumour types. 23 of the 25 tumours that recurred harboured an MDM2 amplification and the average size of the tumours that recurred was 18 cm (range 12-24.5 cm).

Conclusions: We found that using FISH to identify MDM2 amplification significantly improved distinguishing lipomas from ALT/WDL. Furthermore, correlation of MDM2 copy number with histological findings subsequently improved diagnostic accuracy.

56 Anti-Angiogenic Factor Endostatin in Osteosarcoma

H-S Kim, S-J Lim, Y-K Park. Kyung Hee Medical Center, School of Medicine, Kyung Hee University, Seoul, Korea; East-West Neo Medical Center, School of Medicine, Kyung Hee University, Seoul, Korea.

Background: Endostatin (ES) is a potent inhibitor of angiogenesis. The expression of ES has not yet been examined in osteosarcoma (OSA). The aim of this study was to analyze the expression of endostatin (ES) and to determine if there is a correlation between the expression of ES and clinicopathological parameters, patient outcomes and/or VEGF expression in OSA.

Design: We made tissue microarrays from 46 cases of OSA and analyzed the expression of ES by immunohistochemistry. A sample was defined as positive when 35% or more of the tumor cells stained positively throughout the tumor core.

Results: Endostatin was expressed in 26.1% (12/46). The expression of ES was significantly correlated with histological grade ($P = .008$), stage ($P = .042$) and distant metastasis ($P = .011$). In contrast, there was no significant correlation between the expression of ES and age ($P = .516$), tumor size ($P = .214$), soft tissue extension ($P = .498$), Huvos grade ($P = .547$) and VEGF expression ($P = 1.000$). Difference in ES expression among primary sites ($P = .375$) or histological subtypes ($P = .571$) was not significant.

Conclusions: Our results suggest that the expression of ES can be used a prognostic factors in OSA patients.

57 Overexpression of TLE1 Is a Robust Biomarker for Synovial Sarcomas and Correlates with t(X;18): Analysis of 373 Cases

Th Knosel, S Heretsch, A Altendorf-Hofmann, P Richter, K Katzenkamp, D Katzenkamp, A Berndt, I Petersen. Friedrich-Schiller University, Jena, Germany.

Background: Genomewide expression profiling has identified a number of genes expressed at higher levels in synovial sarcoma than in other sarcomas. Our objectives in this study were: 1) to test whether the differentially expressed gene, TLE1, is also distinct on the protein level 2) to evaluate this biomarker in a series of well characterized synovial sarcomas 3) to correlate the overexpression of TLE1 with t(X;18) and other established biomarkers.

Design: 373 spindle cell sarcomas from the German consultation and reference center of soft tissue tumors initially suspected for synovial sarcoma were revisited. Of these 202 specimens were analyzed immunohistochemically using the antibody TLE1. The staining was scored semiquantitatively as -, negative; +, weak; ++, moderate; and +++, strong positive. Furthermore, of these 118 specimens were analyzed using FISH and/or PCR to detect t(X;18) SYT-SSX translocation. We correlated the TLE1 overexpression with the translocation status and the other established biomarkers (EMA, PanCK, CD34, bcl2).

Results: TLE1 overexpression was observed in 96.5% of the synovial sarcomas (score $\geq +$) and discriminates them from other soft tissue spindle cell tumors ($p < 0.001$). Multivariate analysis showed that positive TLE1 and negative CD34 staining were statistically independent diagnostic markers. Furthermore molecular analysis showed that t(X;18) were clearly correlated with overexpression of the gene TLE1 ($p < 0.001$).

Conclusions: Overexpression of TLE1 is significantly correlated with t(X;18) and may serve in synovial sarcomas as a new powerful diagnostic biomarker and potential therapeutic target.

58 Immunohistochemical Comparative Study of Chondromyxoid Fibroma, Chondroblastoma and Chondrosarcoma, Using Sox9, p63 and CAM 5.2

E Konishi, Y Nakashima, Y Iwasa, A Yanagisawa. Kyoto Prefectural University of Medicine, Kyoto, Japan; Kyoto University Hospital, Kyoto, Japan; National Hospital Organization Osaka Medical Center, Osaka, Japan.

Background: Recently, some antibodies are thought to be useful makers for differential diagnosis of the bone tumors. Sox9, an essential regulator of chondrogenesis can

immunohistochemically distinguish mononuclear cells of mesenchymal chondrosarcoma from other small blue round cell tumors, including Ewing sarcoma/PNET. Some cytokeratins, such as CK8, CK18, and CK20 are expressed in chondroblastoma (CB) but not in chondromyxoid fibroma (CMF). Furthermore, p63 can differentiate mononuclear cells in giant cell tumor from those in other lesions, such as CB, brown tumor, etc. To elucidate the characteristics of CMF, CB and conventional chondrosarcoma (CS), we performed immunohistochemical analysis of Sox9, S-100, type II collagen, CD10, p63, and CAM5.2 (mixture of CK8+CK18).

Design: Ten CMFs, six CBs and eight CSs were studied. Immunohistochemical expression of Sox9, S-100, type II collagen, CD10, p63, and CAM5.2 was analyzed in each case. All antibodies were commercially available.

Results: Positivity of immunostaining is shown in the Table.

	Results of Immunostaining (positive number)					
	Sox9	S-100	type II collagen	CD10	p63	CAM5.2
CMF (n=10)	10/10	5/10	7/10	3/10	6/10	1/10
CB (n=6)	6/6	6/6	4/6	0/6	6/6	6/6
CS (n=8)	8/8	8/8	8/8	0/6*	0/8	0/8

*Some specimens floated off the glass slides. ♥: p<0.05, ♦, ▲: p<0.01

Sox9 was detectable in the nuclei of CMFs, CBs and CSs, even in only focal area. Positive cells were usually in the myxoid or chondroid matrix. S-100 was found in the nuclei and/or cytoplasm of CBs and CSs. Half cases of CMFs were positive for S-100. Myxoid or chondroid matrix of most CMFs, CBs, and CSs was positive for type II collagen, even in focal area. CD10 was occasionally positive in the tumor cells at the periphery of the chondromyxoid lobules of CMFs, however, was negative in those of CBs and CSs. p63 was positive in the nuclei of CBs and sometimes positive in CMFs but not in CSs. CAM 5.2 was positive in all CBs, but in only one CMF. It was negative in CSs.

Conclusions: 1) CMF was verified as chondrogenic tumor in terms of the positivity of Sox9, as well as type II collagen. 2) CMF occasionally contained CD10 positive tumor cells, but CB and CS did not. 3) p63 might be a useful marker to distinguish CS from CB and CMF. 4) CAM5.2 could differentiate CB from CMF and CS.

59 Heterotopic Bone in Epithelioid Sarcomas: A Histopathological Review of 4 Cases

SA Koplin, GP Nielsen, AE Rosenberg. Massachusetts General Hospital, Boston, MA.

Background: Epithelioid sarcoma is an uncommon malignancy which usually arises in the superficial soft tissues of the extremities. Classically, epithelioid sarcomas grow as nodules of moderately atypical epithelioid cells with central necrosis. The stroma is variably fibrous and rarely may contain heterotopic bone. The presence of bone within epithelioid sarcoma has received little attention in the literature.

Design: We reviewed our surgical pathology files from 1987 to 2008 and identified 91 cases of epithelioid sarcoma. Four tumors contained heterotopic bone and they formed the study group. Histologic sections from these four cases were reviewed, and the heterotopic bone was characterized by location (peripheral versus central), architecture (woven versus lamellar) and type (cancellous versus cortical-like). We also noted the presence or absence of prominent osteoblastic rimming, cartilage and mineralization.

Results: The results are summarized Table 1. The diagnosis of epithelioid sarcoma was confirmed by morphology, immunohistochemistry and ultrastructural analysis, when available. Analysis of the heterotopic bone revealed predominantly woven bone which was located both centrally and peripherally. The majority of the woven bone was trabecular in architecture, but cortical-like bone was identified as well as small foci of mature lamellar bone. Osteoblastic rimming was variable and ranged from minimal to prominent. The bone was generally mineralized and small foci of cartilage with enchondral ossification were present in two of the tumors

Patient Data

Patient	Age	Location	Size (cm)	Location of Bone	Architecture of Bone	Type of Bone	Osteoblastic Rimming
1	40	Forearm	11	Peripheral and central	Woven	Trabecular	Prominent
2	5	Base of Skull	Unknown	Peripheral and central	Woven, focal lamellar	Trabecular	Minimal to focally prominent
3	45	Forearm	4.5	Predominantly peripheral, focal central	Woven, focal lamellar	Trabecular, focal cortical-like	Minimal
4	27	Forearm	11	Peripheral and central	Woven, focal lamellar	Trabecular	Minimal

Conclusions: Epithelioid sarcomas infrequently contain heterotopic bone. When present, the bone may be located throughout the mass, is largely woven in architecture and trabecular in configuration, is often rimmed by osteoblasts and is mineralized. The presence of heterotopic bone raises a broad differential diagnosis including both non-neoplastic, reactive tumors such as myositis ossificans as well as benign and malignant neoplasms including ossifying fibromyxoid tumor, synovial sarcoma and osteosarcoma.

60 TLE1 Expression Is Not Specific for Synovial Sarcoma: A Standard Section Study of 155 Soft Tissue and Bone Neoplasms

K Kosemehmetoglu, JA Vrana, AL Folpe. Hacettepe University Faculty of Medicine, Ankara, Turkey; Mayo Clinic, Rochester, MN.

Background: TLE1, a transcriptional repressor essential in hematopoiesis, neuronal differentiation and terminal epithelial differentiation, has recently been shown in a single tissue microarray (TMA) study to be a highly sensitive and specific marker of synovial sarcomas. Expression of TLE1 has not, however, been studied in standard sections of soft tissue and bone tumors. We investigated TLE1 expression in a large series of well-characterized mesenchymal tumors, in order to more fully characterize the range of TLE1 expression.

Design: Standard sections of 155 bone and soft tissue tumors were immunostained for TLE1 (sc-9121, 1:100, Santa Cruz) with Dako Background Reducing Diluent, pretreatment in the Dako PTLINK module with EDTA pH 8.0 for thirty minutes @97 degrees C, and Dako Dual Envision+ detection with Dako DAB+ chromogen. Nuclear positivity was scored as negative (<5% of cell positive), 1+ (5-25% of cells positive), 2+ (25-50% of cells positive), and 3+ (>50% of cells positive).

Results: Overall, TLE1 was expressed at 2-3+ in 48 of 155 (31%) tumors, including 14 of 17 (82%) synovial sarcomas. However, 2-3+ TLE1 expression was also seen in 9 of 11 (82%) schwannomas, 2 of 9 (22%) neurofibromas, 4 of 11 (36%) malignant peripheral nerve sheath tumors, 5 of 13 (38%) rhabdomyosarcomas, 7 of 24 (29%) liposarcomas, 2 of 3 (67%) endometrial stromal sarcomas, 2 of 6 (33%) epithelioid sarcomas, 1 of 4 (25%) solitary fibrous tumors, 2 of 5 (40%) undifferentiated pleomorphic sarcomas, 1 of 5 (20%) leiomyosarcomas, and 1 of 8 (13%) lipomas. TLE1 expression was absent in all cases of alveolar soft part sarcoma, chordoma, clear cell sarcoma, Ewing sarcoma, fibrosarcoma, fibroma, gastrointestinal stromal tumor, low grade fibromyxoid sarcoma, myxofibrosarcoma and myoepithelioma.

Conclusions: Our study confirms the excellent sensitivity of TLE1 for synovial sarcoma. However, TLE1 expression is by no means specific for synovial sarcoma, being present in a number of tumors which enter its differential diagnosis, in particular tumors of peripheral nerve sheath origin. Heterogeneity of TLE1 expression likely explains the differences between the present standard section study and the prior TMA study. TLE1 may be of value in the differential diagnosis of synovial sarcoma, but should be used only in the context of a panel of antibodies. Molecular confirmation of synovial sarcoma-associated fusion genes should remain the "gold standard" for this diagnosis.

61 Diagnostic Utility of Dual-Color Break-Apart Chromogenic In Situ Hybridization for Detection of Rearranged SYT in Formalin-Fixed Paraffin-Embedded Tissue of Synovial Sarcoma

A Kumagai, T Motoi, K Tsuji, T Imamura, T Fukusato. Faculty of Medicine, Teikyo University, Tokyo, Japan; Teikyo University Hospital, Tokyo, Japan.

Background: Synovial sarcoma (SS) consistently carries specific chromosomal translocation t(X;18) and its derivative chimeric genes, either *SYT-SSX1* or *SYT-SSX2*. Detecting these genetic abnormalities by RT-PCR and FISH has been powerful aid for the diagnosis of SS. Recently, chromogenic in situ hybridization (CISH) has gained attention as a newly developed modality that enables simultaneous visualization of both genomic abnormality and the morphology of tumor cells. However, successful use of CISH on the diagnosis of sarcomas has yet to be reported. In this study, we investigated the diagnostic utility of dual-color break-apart CISH as a new method for detecting *SYT* rearrangement in SS.

Design: Formalin-fixed paraffin-embedded tissue samples (FFPEs) from 12 cases of SS and 9 cases of 4 soft tissue sarcomas from which SS need to be distinguished (non-SS). In order to detect *SYT* rearrangement in SS, dual-color break-apart probes were customarily designed at the region adjacent to *SYT*, and were labeled with Texas Red and FITC. After interphase FISH assay, subsequent CISH assay was performed on the same section. For detection of *SYT* rearrangement by CISH and FISH, the numbers of definite split signals were counted in sixty nuclei per sample. *SYT-SSX1* and *SYT-SSX2* fusion status was examined by RT-PCR using RNA extracted from the same FFPEs. The results of CISH, FISH and RT-PCR were correlated.

Results: Positive split signals of *SYT* identified by CISH ranged from 17.5 to 79.2 % (mean 55.2%) in SS, while they were not detected in non-SS. By FISH, split signals were present in 17.5 to 65.0% (mean 39.2%) in SS, but negligible in non-SS (range 0-1.7%, mean 0.2%). These results were consistent with the result of RT-PCR, in which *SYT-SSX1* was detected in 10/12 (83.3%) and *SYT-SSX2* was in 2/12 (16.7%), while fusion genes were not detected in non-SS.

Conclusions: CISH-based *SYT* rearrangement detection system using FFPE provides a highly sensitive and specific method for diagnosis of SS, with the accuracy comparable to FISH and RT-PCR. CISH has several advantages over the FISH and RT-PCR. It circumvents the difficulty to use complicated fluorescence microscope and the unavoidable signal fading of FISH. Unlike RT-PCR, CISH is readily applicable to the FFPEs without influence of poorly preserved RNA. CISH-based method has a great potential for the routine use on the diagnosis of SS.

62 Gain-of-Function PDGFRA Mutations, Previously Reported in Gastrointestinal Stromal Tumors, Are Common in Small Intestinal Inflammatory Fibroid Polyps. A Study on 60 Cases

J Lasota, Z-F Wang, LH Sobin, M Miettinen. AFIP, Washington, DC.

Background: Inflammatory fibroid polyp (IFP) is a rare benign lesion occurring throughout the digestive tract. Usually it is solitary tumor, characterized by a proliferation of highly vascular fibrous tissue infiltrated by inflammatory cells. IFP etiology and histogenesis is not known. Recently, mutations in platelet-derived growth factor receptor alpha (*PDGFRA*) and *PDGFRA* expression have been reported in gastric IFPs. Similar *PDGFRA* mutations were reported in a subset of GISTs.

Design: Sixty well characterized small intestinal IFPs were retrieved from the AFIP files. Expression of *PDGFRA*, KIT, CD34, smooth muscle actin (SMA), desmin and S100 was evaluated immunohistochemically. DNA samples obtained from FFPE tumors were screened for mutations in *PDGFRA* exons 12, 14 and 18 by PCR amplification and direct sequencing of PCR products.

Results: The patient age varied from 13 to 83 years (median 53.5). The male to female ratio was 1:1. Of 32 IFPs 27 were found in the ileum and only 5 in the jejunum. The follow-up data were available in 16 cases; 7 patients were alive (135 to 345 months) with no evidence of the disease, while 9 died of unrelated or unknown causes after 36 to 205 months. Histologically the polyps consisted of an admixture of dendritic-shaped or epithelioid-polygonal mesenchymal cells and inflammatory cells, especially eosinophilic granulocytes. There was a variable collagenous or myxoid extracellular matrix. Strong *PDGFRA* expression was seen in 97 % of IFPs. CD34 was expressed in 11 tumors.

Two IFPs showed SMA expression and one tumor was S100 positive. All IFPs were KIT and desmin negative. *PDGFRA* mutations were identified in 52% of IFPs. There were 25 deletions, 3 deletion-insertions, duplication and single nucleotide substitution in exon 12 and deletion in exon 18.

Conclusions: *PDGFRA* expression and mutational activation is common in the small intestinal IFPs as it is in their gastric counterparts. However, in small intestinal tumors, 97% of mutations were found in exon 12 and only one in exon 18. In contrast, gastric IFPs were previously reported to have predominantly exon 18 mutations. Similar *PDGFRA* mutations were reported in GISTs and are considered a driving force in their pathogenesis. Thus, IFPs should be considered *PDGFRA* driven benign neoplasms.

63 CHOP Is Not Rearranged in Epithelioid Pleomorphic Liposarcoma. Fluorescence In Situ Hybridization (FISH) Study on Four Cases

J Lasota, J Marwaha, JC Fanburg-Smith. Armed Forces Institute of Pathology, Washington, DC.

Background: Epithelioid pleomorphic liposarcoma (EPL), a morphologic subtype of the rare aggressive pleomorphic liposarcoma, has no known consistent chromosomal aberration. Particularly the epithelioid variant, with its sheets of mono- to multivacuolated lipoblasts, may occasionally have morphologic overlap with myxoid/round cell liposarcoma. A case report of EPL demonstrated FUS-CHOP fusion gene transcripts by RT-PCR and postulated it to be part of the myxoid-round cell liposarcoma spectrum, a tumor known to be positive for t(12;16)(q13;p11) resulting in FUS-CHOP fusion gene or less commonly t(12;22)(q13;q12) resulting in EWS-CHOP fusion gene. In this study, additional cases of epithelioid pleomorphic liposarcoma were evaluated for CHOP rearrangements.

Design: Four cases of epithelioid pleomorphic liposarcoma with available block, slides, and folder were retrieved from AFIP files. All tumors were evaluated for CHOP rearrangements using FISH and dual color, break apart CHOP rearrangement probe (Abbott Molecular, US).

Results: Four epithelioid pleomorphic liposarcomas (3M:1F) were included. The patients ranged from 42 to 78 years with a mean age of 60.5 years. Tumor size ranged from 1.5 cm - 15 cm, mean 9.3 cm. Locations included buttock, shoulder, chest, and thigh, the latter with a known metastasis to chest wall. All tumors had sheets of large bizarre monovacuolated to multivacuolated lipoblasts, with necrosis and increased mitotic activity, including abnormal forms. One case demonstrated transition to spindled malignant fibrous histiocytomalike areas. Delicate vasculature, myxoid change, stellate or small round cells were not observed. All tumors were focally positive for S100 protein and negative for pankeratin, CK18, CK8, CK7, CK20, EMA, CD34, and chromogranin. One case had focal reactivity for desmin and HMB45, suggesting a potential immunophenotypic overlap with malignant PEComa. None of the four epithelioid pleomorphic liposarcomas studied by FISH demonstrated CHOP rearrangements.

Conclusions: Although a case report of epithelioid pleomorphic liposarcoma demonstrated FUS-CHOP fusion gene transcripts by RT-PCR and postulated it to be part of the myxoid-round cell liposarcoma spectrum, in our series, epithelioid pleomorphic liposarcoma does not demonstrate CHOP rearrangement by FISH. Based on this genetic finding, epithelioid pleomorphic liposarcoma should be considered separate from the myxoid-round cell liposarcoma spectrum of tumors.

64 Specific Mutations in the B-Catenin Gene (*CTNNB1*) Correlate with Local Recurrence in Sporadic Desmoid Tumors

AJF Lazar, D Tuvin, S Hajibashi, S Habeeb, S Bolshakov, E Mayordomo-Aranda, CL Warneke, D Lopez-Terrada, RE Pollock, D Lev. MD Anderson Cancer Center, Houston; Texas Children's Hospital and Baylor College of Medicine, Houston.

Background: Desmoid fibromatosis is a rare, non-metastatic neoplasm often showing relentless recurrence. Molecular determinants of desmoid recurrence remain obscure. Beta-catenin deregulation is common in sporadic desmoids, with a high incidence of *CTNNB1* (beta-catenin gene) mutations.

Design: We evaluated *CTNNB1* mutations in a large cohort of sporadic desmoids and examined whether mutation type was relevant to desmoid outcomes. Desmoid specimens (195 tumors from 160 patients; 1985-2005) and dermal scars serving as controls were assembled into a clinical data-linked tissue microarray; *CTNNB1* genotyping was performed for a 138 sporadic desmoid subset. Immunohistochemistry for beta-catenin and cyclinD1 was performed. Data was analyzed using Kaplan-Meier and other standard methods.

Results: *CTNNB1* mutations were observed in 117/138 (85%) of desmoids. Three discrete mutations in two codons of *CTNNB1* exon 3 were identified: 41A (59%), 45F (33%), and 45P (8%; excluded from further analysis due to rarity). Five-year recurrence free survival was significantly poorer in 45F-mutated desmoids (23%; $p < 0.0001$) versus either 41A (57%) or non-mutated tumors (65%). Nuclear beta-catenin expression was observed in 98% of specimens; intensity inversely correlated with incidence of desmoid recurrence ($p < 0.01$). Cyclin D1 expression was observed in 34% of primary desmoids; cases with increased nuclear cyclin D1 had higher levels of nuclear b-catenin and lower recurrence ($p < 0.01$).

Conclusions: *CTNNB1* mutations are common in desmoid tumors and may have prognostic and potentially diagnostic applications. Patients harboring *CTNNB1* (45F) mutations are at particular risk for recurrence, and therefore may especially benefit from adjuvant therapeutic approaches. The surprising result of 45F being associated with lower levels of beta-catenin nuclear accumulation and lower cyclinD1 expression may yield additional novel insights into the mechanism and function of this critical pathway.

65 Immunohistochemical Evaluation of MET and RON Expression in Myxofibrosarcomas and the Correlation with Clinicopathological Parameters and Survival

JC Lee, CF Li, HY Huang. National Taiwan University Hospital, Taipei, Taiwan; Chi-Mei Foundation Medical Center, Tainan, Taiwan; Chang Gung Memorial Hospital, Kaohsiung, Taiwan.

Background: Myxofibrosarcoma (MFS) relatively lacks good prognosticator. Our unpublished data from array-based comparative genomic hybridization analysis on 12 tumor specimens and 2 cell lines showed frequent gains in chromosomal 7q spanning regions harboring *c-MET* oncogene. MET expression is known to be associated with "invasive growth pattern" and drugs targeting it are being developed. RON, a homologue to MET, can elicit reciprocal transphosphorylation with MET. Their expression was found to predict poorer prognosis in various human cancers. Our goal is to detect the expression of these two proteins in MFS and evaluate the prognostication power of them.

Design: We retrospectively collected 73 cases of MFS and performed immunohistochemical stain with MET and RON antibodies. The results were correlated with clinicopathological parameters, which, as well as MET and RON expression, were further correlated with overall survival and metastasis-free survival in 62 patients with available follow-up data.

Results: High MET expression (50 cases, 68.5%) was significantly associated with higher FNCLCC grade, higher AJCC stage, higher mitotic rate, more extensive necrosis, less myxoid area ($p < 0.001$ for all above), larger tumor size ($p = 0.001$), positive margin ($p = 0.002$), and deeper site ($p = 0.035$). High RON expression (36 cases, 49.3%) was significantly associated with higher stage ($p = 0.005$), higher mitotic rate ($p = 0.012$), and less myxoid area ($p = 0.027$). Significant positive correlation between expression of MET and RON was also demonstrated ($p < 0.001$, correlation coefficient = 0.451). Univariate analysis revealed that overall survival was significantly correlated with mitoses, margin, depth, and stage, among which only mitoses ($p = 0.0003$, risk ratio [RR] = 27.736) were significant in multivariate analysis; metastasis-free survival was significantly correlated with mitoses, grade, MET expression, depth, stage, necrosis, size, margin, and RON expression, among which only the first four were significant in multivariate analysis ($p = 0.0001, 0.0185, 0.0198, 0.0348$, and $RR = 57.678, 11.764, 11.582, 28.000$, respectively).

Conclusions: Expression of MET, RON or both is common in MFS. While both were insignificant for overall survival, MET expression was predictive of higher rate of metastasis. In addition, mitotic rate was the strongest prognosticator according to this work.

66 Homozygous Deletion of *MTAP* Gene as a Poor Prognosticator in Gastrointestinal Stromal Tumors (GISTs)

CF Li, WW Huang, SC Yu, HY Huang. Chi-Mei Foundation Medical Center, Yung Kung, Taiwan; Buddhist Dalin Tzu Chi General Hospital, Chiayi, Taiwan; Chang Gung Memorial Hospital, Kaohsiung Medical Center, Kaohsiung, Taiwan.

Background: While chromosomal losses on 9p and/or 9q preferentially affect high-risk cases, little is known about the candidate tumor suppressor genes (TSG) implicating GIST progression, except for *CDKN2A/B*. Using 385K array CGH (aCGH), we screened DNA copy number alterations (CNAs) to fine map potential TSGs on chromosome 9 (Chr9) with special attention given to *MTAP* (methylthioadenosine phosphorylase), a TSG frequently co-deleted with *CDKN2A/B*.

Design: To search TSGs as potential prognosticators, aCGH was profiled for 22 GISTs and criteria for evaluating CNAs on Chr9 were those recurrently deleted in $\geq 40\%$ of high-risk samples and but in $< 40\%$ of intermediate-risk and low-risk samples. *MTAP* immunostain was assessed in 306 independent cases on tissue microarrays of primary GISTs, 146 of which were measured for *MTAP* homozygous deletion (HD) by coupling quantitative PCR with laser microdissection. Additionally, 187 cases had known mutation status of *KIT* and *PDGFRA* receptor tyrosine kinase (RTK) genes. *MTAP* gene status was correlated with immunostain, NIH risk level, Ki-67 labeling index (LI), RTK genotypes, and disease-free survival (DFS).

Results: aCGH identified 10 candidate TSGs on 9p and six on 9q. *MTAP* and/or *CDKN2A/B* at 9p21.3 were deleted in 1 intermediate-risk (11%) and 7 high-risk (70%) GISTs, with 2 cases homozygously co-deleted at both loci. *MTAP* HD, present in 25 cases, was significantly associated with poor DFS ($p < 0.0001$, univariately), gastric site ($p = 0.041$), larger size ($p < 0.001$), and higher mitotic rate ($p = 0.008$), Ki-67 LI ($p < 0.001$), and risk level ($p < 0.001$), but not related to RTK genotypes. While *MTAP* HD correlated with its protein loss ($p < 0.001$), GISTs without *MTAP* expression did not necessarily show HD. In multivariate analysis, *MTAP* HD remained independently predictive of adverse outcome ($p = 0.0369$, $RR = 2.166$), along with high risk category ($p < 0.0001$, $RR = 3.202$), Ki-67 LI $> 5\%$ ($p = 0.0106$, $RR = 2.456$), and non-gastric site ($p = 0.0416$, $RR = 1.960$).

Conclusions: *MTAP* HD, present in 17% of GISTs, is one mechanism to deplete its protein expression. It correlates with several prognosticators and independently predicts poor DFS in GISTs, highlighting its role in disease progression. *MTAP* HD may also provide a target of alternative therapy for GISTs, since cells with this change are susceptible to *MTAP*-directed agents, such as L-alanosine.

67 Quantitative Analysis of Activating Alpha Subunit of the G Protein Mutation by Pyrosequencing for Fibrous Dysplasia

Q Liang, MQ Wei, GH Wang, JC Fanburg-Smith, A Nelson, M Miettinen, RD Foss. Armed Forces Institute of Pathology, Washington, DC.

Background: Benign fibro-osseous lesions (BFOL) frequently display overlapping histologic features. Differentiation of fibrous dysplasia (FD) from other BFOL can be difficult, even for experienced orthopedic pathologists. A somatic mutation at codon Arg²⁰¹ of the alpha subunit of the G protein has been identified in FD and is specifically absent in other BFOL. A sensitive quantitative method could potentially eliminate some of the uncertainty in the diagnosis of these BFOL. We have developed a quantitative

assay using a pyrosequencing method which has a detection sensitivity of at least 5% of affected cells admixed with normal tissue. The test allows the identification of 2 most common types of mutation (Arg to His and Arg to Cys), along with the rare Arg to Leu mutation, in a single run.

Design: Twenty-five FD, 2 osteofibrous dysplasia (OD), 9 ossifying fibromas (8 gnathic and 1 metacarpal), 4 BFOL not otherwise specified, 2 desmoplastic fibroma, and 7 Paget Disease cases from our files were selected. Sequencing analysis by pyrosequencing was performed on formalin fixed, paraffin embedded tissue from these cases. Histological and immunohistochemical features (if applicable) and clinical histories were reviewed.

Results: Of the 25 FD cases, 23 (92%) were positive for alpha subunit of the G protein mutation. Nineteen of 23 positive cases have a G->A mutation (Arg->His) and 4 have a C->T mutation (Arg->Cys). Two of 4 cases of BFOL not otherwise specified cases were positive for G->A mutation. None of osteofibrous dysplasia, ossifying fibroma, desmoplastic fibroma, and Paget Disease cases were positive for this mutation.

Conclusions: Mutation analysis of the alpha subunit of the G protein by pyrosequencing has significant potential for improving discrimination between FD and other BFOL in problematic cases. Compared to other detection methods such as restriction enzymatic digestion and probe hybridization, pyrosequencing has the ability to identify several types of mutations in a single reaction. In addition, pyrosequencing method achieves greater quantification sensitivity than general sequencing. In combination with microdissection techniques, the quantification ability of pyrosequencing may enable us to correlate the mutation detection with histopathological events. We believe that pyrosequencing is a relatively easy and accurate method for activating alpha subunit of the G protein mutation detection and quantification in fibrous dysplasia.

68 Giant Cell Lesions of Bone and Soft Tissues: Diagnostic Value of Immunohistochemistry

MD Linden, Henry Ford Hospital, Detroit, MI.

Background: Giant cell lesions of bone and soft tissues are a heterogeneous group. This includes both benign and malignant tumors with a broad range of clinical behaviors. Accurate diagnosis is essential for determination of prognosis and guiding treatment decisions. Clinicians are more frequently submitting needle core biopsy and fine needle aspiration specimens of mesenchymal lesions, often providing only limited amounts of lesional tissue for diagnosis. Immunohistochemistry may be a useful ancillary tool to discriminate giant cell tumor of bone from other giant cell rich lesions, especially on specimens with limited cellularity.

Design: A group of giant cell rich lesions of bone and soft tissue were selected from the surgical pathology archives at Henry Ford Hospital. Cases included the following- giant cell tumor of bone (5), giant cell tumor of tendon sheath (20), pigmented villonodular tenosynovitis (10), phosphatitic mesenchymal tumor, mixed connective tissue variant (1), and aneurysmal bone cyst (4). An immunohistochemistry panel was performed consisting of p63, CD 34, CD 68, CD 117, and CD 163. Immunoreactivity of cases was scored as "negative", "focal positive" (<5%), and "positive" (>5%). Lesional component staining was also recorded as to specific cell population, stromal cells and/or giant cells.

Results: All cases (5/5) of giant cell tumor of bone were immunoreactive with p63. Both stromal cells and giant cells. CD163 showed variable staining of both stromal cells and giant cells. CD68 stained only giant cells. CD34 and CD117 were negative. Similar staining patterns were observed with aneurysmal bone cyst. 4/4 cases were p63 positive. All cases of giant cell tumor of tendon sheath and pigmented villonodular tenosynovitis were p63 negative. In contrast, both CD68 and CD163 showed immunoreactivity of both giant cells and stromal cells. CD34 and CD117 were negative. The one case of phosphatitic mesenchymal tumor was negative with all of the immunostains.

Conclusions: We observed p63 immunostaining only in cases of giant cell tumor of bone and aneurysmal bone cyst, findings similar to previous reports in the literature. CD68 and CD163 staining appeared restricted to giant cell tumor of tendon sheath and pigmented villonodular tenosynovitis. CD34 and CD117 were non-contributory in this series of cases. These patterns of immunoreactivity may be useful to discriminate giant cell tumor of bone (p63 positive) from other giant cell rich lesions of bone and soft tissue such as GCTTS and PVNS (p63 negative), especially on limited samples.

69 Retroperitoneal Lipoma: A Clinicopathology and Molecular Study of 16 Cases

RS Macarenco, MR Erickson-Johnson, X Wang, AL Folpe, BP Rubin, AG Nascimento, MF Franco, AM Oliveira. CIPAX, Sao Paulo, Brazil; Mayo Clinic, Rochester, MN; Cleveland Clinic, Cleveland, OH; UNIFESP, Sao Paulo, Brazil.

Background: In the retroperitoneum, well-differentiated liposarcomas (WDL) vastly outnumber benign adipocytic neoplasms. Indeed, in many institutions, all retroperitoneal adipocytic tumors have been traditionally classified as WDL, even when they lack diagnostic cytologically atypical cells. Recently, we have reported a well-characterized retroperitoneal lipoma (RL) with classic cytogenetic and molecular genetic features (Am J Surg Pathol 2008; 32: 951-954). Herein we expanded those initial observations to a large series of RL to better understand their clinico-pathologic and molecular characteristics using strict morphologic and genetic criteria.

Design: Sixteen cases of RL were identified at Mayo Clinic, both from internal material (n=6) and our consultation practice (n=10). All cases were extensively sampled and reviewed by three soft tissue pathologists. Fresh tissue material was available from five cases for standard cytogenetic analysis. Molecular cytogenetic studies for *MDM2*, *CPM*, *SAS*, *CDK4*, *CHOP* and *HMG2* were performed in all cases using FISH. RT-PCR was performed in 6 cases. Follow-up information was obtained in 10 instances.

Results: There were 8 females and 6 males, ranging from 36-73 years of age (median 57 years). All tumors were located in the retroperitoneum. Median tumor size and weight were 22 cm (range, 8-32 cm) and 1127g (range, 173-2440g), respectively. Histologically, all tumors were composed of mature adipose tissue without cytologic atypia. Standard cytogenetic analysis showed rearrangements of 12q15 in 3 (of 5) cases. None showed

ring/giant marker chromosomes or complex karyotypes. FISH showed no amplification of *MDM2*, *CPM*, *SAS*, *CDK4*, *CHOP* or *HMG2* in all 16 cases. *HMG2* rearrangement was observed in 6 (of 16) cases (38%). Among these, the fusion gene *HMG2-LPP* was seen in only one case. All tumors were completely resected, and none recurred or metastasized after 1-58 months (median, 7 months).

Conclusions: RL occur in older adults and may attain large size at diagnosis but seem to follow an uneventful clinical course if completely resected. Cytogenetic and/or molecular genetic study are required for the diagnosis of RL in this anatomical location, given the overwhelming preponderance of WDL. Additional clinical follow-up will be required to completely understand the natural history of RL.

70 Dedifferentiated Solitary Fibrous Tumors: A Clinicopathologic Study of 7 Cases

RS Macarenco, MR Erickson-Johnson, X Wang, AG Nascimento, AL Folpe, AM Oliveira. CIPAX-Medicina Diagnostica, Sao Jose dos Campos, SP, Brazil; Mayo Clinic, Rochester, MN.

Background: Solitary fibrous tumor (SFT) is a fibroblastic neoplasm. Histological features associated with malignant behavior include high cellularity, mitotic activity (>4/10 HPF), nuclear pleomorphism, necrosis, size >5 cm, and infiltrative tumor borders. Clinicopathologic features of "dedifferentiated SFT" (DD-SFT), defined as high grade undifferentiated sarcoma juxtaposed to a histologically classic SFT, have not been described in detail.

Design: Seven DD-SFT were retrieved from our archives. Histological slides were reviewed; immunohistochemistry and ploidy digital image analysis were performed when possible. Clinical information including treatment and follow-up were added.

Results: Cases occurred in 4M and 3F, with a median age of 64ys (range 49-73 ys). Sites included lung, axilla, thigh, upper back, paratestis, and scalp. Median tumor size was 9 cm (range 4-10 cm). All cases had areas of histologically typical SFT juxtaposed to malignant areas. Six cases had abrupt transition between typical and DD-SFT, whereas in one case the components were intermixed. Dedifferentiated areas comprised 10 to 95% of each case and consisted of pleomorphic sarcoma (5 cases), pleomorphic sarcoma of the inflammatory type (1 case), and undifferentiated sarcoma with an epithelioid and pseudo-alveolar pattern (1 case). Cellularity, nuclear atypia and pleomorphism, and mitotic activity were higher in the DD areas (mean=102/50 HPF) as compared to the more typical areas (mean=48/50HPF). Tumor necrosis and vascular invasion were identified in the DD component of two cases. All cases showed diffuse CD34 expression in areas of typical SFT; DD areas showed uniformly retained (4 cases), partially retained (1 case) and absent (1 case) CD34 expression. All tumors were negative for S100 protein, smooth muscle actin, desmin and cytokeratin. DIA showed aneuploidy in both areas in 4 (of 4) cases evaluated. Outcome (available in 4) showed that 2 patients presented with metastatic disease (1 died 1 month after diagnosis and the other was well 1 month after surgery), 1 patient was alive with local recurrence 3.5 years after diagnosis, and one patient free of disease 2 years after diagnosis.

Conclusions: Dedifferentiation represents a rare form of progression in SFT. Additional cases are necessary to more fully understand their natural history. Follow-up to date suggests behavior more aggressive than conventional malignant SFT, akin to other types of dedifferentiated sarcoma.

71 Massive Localized Lymphedema: A Clinicopathological Study of 21 Cases of a Still Poorly Recognized Pseudosarcoma Occurring in Morbidly Obese Patients

M Manduch, AM Oliveira, AG Nascimento, AL Folpe. Mayo Clinic, Rochester, MN.

Background: Massive localized lymphedema (MLL) is a rare, relatively recently described pseudosarcoma most often occurring in morbidly obese patients. Owing to its rarity, MLL remains poorly recognized. In this large series of cases we further expand the spectrum of clinicopathologic features of this unusual entity, and emphasize its differential diagnosis from soft tissue neoplasms of various types.

Design: We performed a retrospective review of all cases diagnosed as MLL. All H and E stained sections were reviewed. Clinical information was obtained from the referring pathologists and clinicians.

Results: 21 morbidly obese adults (mean patient weight 186 kg/ 411 lb.) presented with unilateral, large soft tissue lesions of longstanding duration. The clinical history was also notable in 3 patients for previous inguinal herniorrhaphy, multiple surgeries for scrotal edema, and hemiparesis secondary to gunshot trauma. Most lesions involved the proximal medial thigh (9) or thigh (6), but also occurred in the distal medial thigh (1), posterior thigh (1), posterior calf (1) and lower leg (3). Clinically, most lesions were regarded as representing benign processes, including pedunculated lipoma (6), lymphocele (1) or recurrent cellulitis (4), although soft tissue sarcoma was also suspected in 2 cases. Pathologists, however, regarded the majority of cases as potentially malignant, with suggested diagnoses including well-differentiated liposarcoma (WDL, 10), myxoid liposarcoma (1), and angiosarcoma (1). Grossly, all masses showed "peau d'orange" skin changes, and were ill-defined, unencapsulated, lobulated, and very large (mean size 31 cm, range 15 - 61.5 cm, mean weight 3386 gm, range 1133 - 10800 gm). Histologically, all 21 cases demonstrated striking dermal fibrosis, expansion of the fibrous septa between fat lobules with increased numbers of stromal fibroblasts, lymphatic proliferation and lymphangiectasia. Multinucleated fibroblastic cells (4), marked vascular proliferation (5), moderate stromal cellularity (4) and fascicular growth raised concern among referring pathologists for WDL, angiosarcoma, and a fibroblastic neoplasm in 10, 1, and 1 cases, respectively.

Conclusions: Many cases of MLL continue to be misdiagnosed by clinicians and pathologists as various types of soft tissue neoplasms, in particular WDL. Awareness of this entity, clinical correlation and gross pathological correlation are essential in the distinction of this distinctive pseudosarcoma from its various morphological mimics.

72 Gastrointestinal Stromal Tumors (GISTs) of the Omentum – A Clinicopathologic Study of 95 Cases

M Miettinen, LH Sobin, J Lasota. Armed Forces Institute of Pathology, Washington, DC.

Background: GISTs, KIT-positive and oncogenic KIT/PDGFR mutation-driven mesenchymal neoplasms, most commonly originate from the stomach or small intestine, but a small number of GIST is believed to primarily involve the omentum. Mutation status, histology, and long-term prognosis of omental GISTs are poorly understood.

Design: We analyzed 95 GISTs that were surgically designated as omental tumors. Immunohistochemical studies were performed to evaluate KIT, CD34, and SMA expression. KIT and PDGFRA mutations were analyzed on 37 cases following PCR amplification and direct sequencing. Histologic features, tumor size, single vs. multiple tumors, and follow-up status were analyzed.

Results: There were 46 females and 49 males of ages 48-88 yrs (median, 60 yrs). KIT mutations were detected in 15 cases (12 in exon 11 with 7 deletions, 4 substitutions, 1 duplication; 3 exon 9 duplications). PDGFRA mutations were detected in 11 cases (9 in exon 18, 2 in exon 12), and wild-type for both genes in 11 cases. The tumors were single in 52 cases, multiple in 38 cases, and indeterminate in 5 cases. The two first groups were analyzed for selected factors. Single tumor cases showed the following: KIT+ 40/43, CD34+ 21/35, SMA+ 12/38, mitoses median 3/50 HPFs, tumor size median 14 cm, median survival of 120 months (range, 0-397 months). 39 tumors had histological features typical of gastric GISTs, and 13 of small intestinal GISTs. Ten of the single tumors were attached to stomach, and 5 of these patients were alive at the end of follow-up (median survival time for living patients, 235 months). Multiple tumor cases showed: KIT+ 22/23, CD34+ 7/20, SMA+ 3/21, mitoses median 11/50, tumor size median 17 cm, median survival 8 months (all died). 20 tumors had histologic features of small intestinal and 18 of gastric GISTs.

Conclusions: Omental GISTs are a heterogeneous group. A majority of tumors presenting as single tumors have features of gastric GISTs, and high frequency of PDGFRA mutants support common gastric origin for these tumors. Omental GISTs include a small prognostically favorable subgroup: single GISTs attached to stomach of gastric origin forming a dominant omental mass. Also, patients with low mitotic rates have a longer survival. Multiple tumor presentation has a poor prognosis, and GISTs with features of small intestinal ones cluster in this group. All omental GISTs probably primarily originate from the GI tract.

73 The Effect of Radiation/Chemotherapy on the Immunophenotype of Soft Tissue Sarcomas

EC Miller, MA Stevenson, MC Gebhardt, ME Anderson, JD Goldsmith. Beth Israel Deaconess Medical Center, Boston, MA; Harvard Medical School, Boston, MA.

Background: Many sarcoma centers treat with chemotherapy and radiation prior to definitive excision of intermediate or high grade soft tissue sarcomas (STS); this therapy is anecdotally thought to modify the immunophenotype of these tumors, thus making interpretation of immunohistochemical studies difficult in a post-therapy excision specimen. To our knowledge, however, there is no study that has systematically evaluated the effects of radiation and/or chemotherapy on the immunophenotype of STS.

Design: Patients with pretreatment core or incisional biopsies and post treatment excisions were found by searching the patient database in the department of radiation oncology. Both pre-therapy biopsies and post-therapy excisions were stained in the usual manner with common immunohistochemistry (IHC) stains used in STS (S-100, smooth muscle actin, desmin, screening cytokeratin [AE1-3/CAM 5.2], cytokeratin MNF116, CD34, and HMB45). Stains were examined blindly and separately and categorized as negative, 1+ (<10%), 2+ (10-50%), 3+ (50-100%) based on the fraction of tumor cells that were positive.

Results: Eleven patients with pre-treatment biopsies and post-treatment excisions were analyzed. Mean patient age at original diagnosis was 52 years (range 24-77 years). The female to male ratio was 2.8:1. There were 7 pretreatment core biopsies and 4 pretreatment incisional biopsies. 42 pairs of IHC stains were examined in total. If 1+ and negative, and 2+/3+ were grouped and compared, all pre and post-treatment results correlated except for 7 pre/post-treatment stain pairs (83%). However, if the negative and 1+ results were considered separately, 29 of 42 stain pairs (69%) showed correlation. The stains that did not correlate were not limited to particular antibodies.

Conclusions: The immunophenotype of STS shows some fidelity after treatment with chemotherapy and radiation. Based on the results of this pilot study, immunohistochemistry might be used with caution on tissue exposed to radiation and/or chemotherapy.

74 Advantage of FISH Analysis Using PDGFB Dual-Color, Break-Apart Probes for an Adjunct to Diagnosis of Dermatofibrosarcoma Protuberans

T Mitsuhashi, H Asanuma, T Matsumura, N Tochigi, T Shimoda, T Hasegawa. Sapporo Medical University, Sapporo, Japan; National Cancer Center Hospital and Research Institute, Tokyo, Japan.

Background: Dermatofibrosarcoma protuberans (DFSP) represents a low-grade mesenchymal neoplasm of fibroblast/myofibroblast, and it occasionally contains fibrosarcoma (FS) component. Cytogenetically, all forms of DFSP are characterized by t(17;22)(q22;p13) translocation, with some cases resulting in supernumerary ring chromosomes. This translocation fuses the collagen type I $\alpha 1$ (*COL1A1*) gene to the platelet-derived growth factor β -chain (*PDGFB*) gene. While many *CAL1A1* gene breakpoints have been identified, *PDGFB* gene breakpoint is remarkably constant. In this study, we investigate the advantage of fluorescence in-situ hybridization (FISH) using newly developed dual-color, break-apart (NDDCBA) probes for *PDGFB* at diagnostic laboratories for the application to pathological diagnosis and therapeutic interventions.

Design: Formalin-fixed paraffin-embedded (FFPE) tissues from 13 DFSP (including FS in 3 cases) and 13 control superficial spindle cell tumors were used. The expression of CD34 and PDGFB receptor (PBGFRB) were evaluated immunohistochemically, and FISH analysis was performed using NDDCBA probes for *PDGFB*. In FISH analysis, only distinct split signals were counted in 50 tumor cells, and the results were regarded as positive if more than 10% of tumor cells show split signals, green (G) and orange (O). In addition, it was regarded as amplification if extra signals were observed, and amplification rate was calculated by 50 tumor cells.

Results: Immunohistochemically, all DFSP were CD34+, and all DFSP and FS component were PDGFRB+, either diffusely or focally. In FISH analysis for *PDGFB*, signals were detected in 9 of 13 cases of DFSP (with or without FS), and in 11 of 13 cases of control.

Results of FISH Analysis

	Split signals (%)	G/O ratio (mean)	Amplification rate in % (mean)
DFSP (n=9)	9/9 (100)	1.47-3.3 (2.22)	70-90 (80)
FS (n=3)	3/3 (100)	1.51-2.0 (1.70)	72-94 (82)
Control (n=11)	0/0 (0)	0.95-1.02 (0.99)	0-14 (7.6)

Conclusions: FISH analysis using NDDCBA probes for *PDGFB* was enabled by FFPE DFSP tissues. Its detection is particularly helpful in the differential diagnosis of atypical, fibrosarcomatous, and metastatic DFSP, and may be useful to evaluate the application of imatinib to non-resectable, recurrent and metastatic DFSPs.

75 Homozygous Deletion of CDKN2 in Tumorigenic Mesenchymal Stem Cells: A Key Event for Osteosarcoma Genesis

AB Mohseny, K Zuhai, S Romeo, EP Buddingh, I Briaire-de Bruijn, D de Jong, M van Pel, PCW Hogendoorn, AM Cleton-Jansen. Leiden University Medical Center, Leiden, Netherlands.

Background: Osteosarcoma (OS) is a malignant bone tumour in which associations with underlying hereditary diseases or germline mutations are limited. Given the young age of occurrence, a sequential accumulation of carcinogenic hits for malignant transformation is unlikely. Moreover, OS is characterized by extreme genetic instability. So identification of its cell of origin is crucial for characterizing genetic events responsible for OS formation and identifying alternative therapeutic targets. Potential cells of origin are mesenchymal stem cells (MSCs), given their role in normal bone remodeling during growth spurt and their multipotential differentiation commitment evoking the histological spectrum observed in OS. Accordingly we investigated murine MSCs as a model for OS formation.

Design: OS deriving murine MSCs were characterized at different stages, i.e. genetically (COBRA-FISH, arrayCGH), mRNA expression (qRT-PCR), phenotypically (FACS) and functionally (differentiation, adhesion-independency and tumour formation) to recapitulate OS formation upon malignant transformation of MSCs. Findings were verified on a clinical series of 144 OS cases, including biopsies, resections and metastases.

Results: Long-term *in vitro* culturing induced remarkable changes: aneuploidization, loss of *CDKN2* locus, loss of *CDKN2A/p16* gene expression, anchorage independent growth and subcutaneous OS formation in nude mice. Intriguingly, MSC characteristics remained as substantiated by specific markers expression and they retained capacity to differentiate towards osteoblasts, chondroblasts and adipocytes. On a clinical series, expression levels of the *CDKN2A/p16* protein showed a significant correlation with patients survival (logrank, $p < 0.000$).

Conclusions: Here we established a unique and reproducible model to study different steps in OS genesis. As compared to full blown OS this model allows far better detection of driving genetic mechanisms. Furthermore this model provides substantial evidence for a MSCs origin of OS and identifies *CDKN2* deletion as a key event. The importance of loss of *CDKN2A* expression is clinically validated by its ability to predict survival better than the currently used response to chemotherapy.

76 Radiation-Associated Sarcoma of Soft Tissue and Bone: A Clinicopathologic Study of 70 Cases in a Single Institution

EA Morgan, DE Kozono, JE Butrynski, EH Baldini, CP Raut, AF Nascimto. Brigham and Women's Hospital (BWH), Boston, MA; BWH and Dana-Farber Cancer Institute (DFCI), Boston; DFCI, Boston; BWH, Boston.

Background: Development of sarcomas is a rare but serious complication of radiation therapy (RT). Cutaneous angiosarcoma of the breast following radiation for conservative treatment of breast carcinoma is the best described radiation-associated sarcoma (RAS). Sarcomas arising in other sites are poorly characterized.

Design: We reviewed all cases of RAS evaluated at our institution from 1987 to 2008. RT-associated breast angiosarcomas were excluded. Clinicopathologic data were obtained by medical record review. Survival was analyzed by Kaplan-Meier curve.

Results: 70 patients (pts) (51 female, 19 male) were identified, with a mean age at RAS diagnosis of 53 yrs. Primary diseases were invasive breast cancer (18 cases), Hodgkin lymphoma (14), cervical cancer (6), non-small cell lung cancer (3), endometrial cancer (3), head and neck squamous cell cancer (3), DCIS (2), Ewing's sarcoma (2), embryonal rhabdomyosarcoma (2), seminoma (2), non-Hodgkin lymphoma (2), rectal cancer (2), thyroid cancer, prostate cancer, Wilms' tumor, CML, retinoblastoma, endometriosis and desmoid tumor (1 each). Four pts received RT to the same site for two distinct primaries greater than a year apart. Median interval between RT and RAS was 168 mos (range 36 to 552). In 60% of cases, pts noticed symptoms at a median of 3 mos before diagnosis. RAS diagnoses were leiomyosarcoma (10 cases), MPNST (6), osteosarcoma (6), angiosarcoma (2), and unclassified sarcoma (46). The majority of the tumors (68%) were histologically high grade. Cytogenetic analysis (18 cases) demonstrated complex karyotypes without recurrent abnormalities. Surgical resection was performed in 56 cases followed by chemotherapy and/or RT in 21 cases. 21% of pts developed recurrence and 17% developed metastasis (median 8 and 22 mos after RAS, respectively). 49% of pts died of disease and the 5-year survival was 38%.

Conclusions: Most RAS are unclassified, high grade sarcomas. The majority have complex karyotypic abnormalities and sarcomas with recurrent translocations do not typically arise in the setting of RT. The cornerstone of therapy is surgery. Although the median latency period is quite long from initial RT administration, prognosis is poor with a 5-year survival of 38%.

77 Expanding the Spectrum of Dedifferentiation in Soft Tissue Tumors: Dedifferentiated Solitary Fibrous Tumor – A Study of 8 Cases

JM Mosquera, CDM Fletcher. University Medical Group, Providence, RI; Brigham and Women's Hospital & Harvard Medical School, Boston, MA.

Background: Dedifferentiation is a well-recognized form of tumor progression in certain types of low grade soft tissue and bone sarcoma, and confers a worse prognosis. To date, dedifferentiation has not been described in solitary fibrous tumor (SFT).

Design: Among 948 cases of intrathoracic and extrathoracic SFTs accessioned between 1988 and 2008, we identified 8 cases of primary dedifferentiated SFT. Immunohistochemistry was performed. Clinical and follow-up information was obtained from the referring pathologists and/or the treating physician.

Results: Dedifferentiated SFT occurred in three men and five women, 40 to 76 years old ($\chi = 59$ years), and measured 3.4 to 20.0 cm ($\chi = 10.6$ cm). Two cases were intrathoracic, two were in deep soft tissue of thigh, and single cases were located in omentum, scalp, retroperitoneum and abdominal wall. In addition to typical features of SFT there was abrupt transition to non-distinctive high-grade sarcoma in all cases. The latter included spindle and/or epithelioid components with increased mitotic activity, necrosis and cystic degeneration. All cases were CD34 positive in the usual SFT areas, while 5 showed loss of CD34 in the poorly differentiated component. Six of 7 cases stained for p53 and p16 showed either negative or scattered positive cells in well-differentiated SFT areas, in contrast to positive or stronger and more diffuse staining in the high-grade component. Follow-up information available in 7 patients ranged from 1 to 58 months ($\chi = 22$ months). Three patients with the largest tumors (20.0, 17.0, and 9.0 cm) died of disease after 1, 8, and 34 months of presentation. Three patients whose tumors measured less than 8.0 cm show no evidence of disease at last follow-up. One patient with an 11.5 cm intrathoracic dedifferentiated SFT is alive with disease at 58 months after recurrence and metastasis.

Conclusions: We describe, apparently for the first time, the phenomenon of dedifferentiation in SFT. Our results demonstrate that this phenomenon, as in other soft tissue tumors, poses a higher risk of tumor recurrence and/or metastasis, particularly in large and deep seated tumors. Similar to other dedifferentiated sarcomas, abrupt transition between low grade and high-grade areas is typically observed. Loss of CD34 positivity, and p53 and p16 overexpression in the high-grade component is common as in other dedifferentiated lesions, perhaps pertaining to the underlying mechanism.

78 Recurrent Chromosomal Copy Number Alterations in Chordoma

GP Nielsen, V Deshpande, AE Rosenberg, JM Batten, F Hornicek, J Iafrate. Massachusetts General Hospital, Boston, MA.

Background: Chordoma is an uncommon neoplasm with the vast majority arising in the axial skeleton. Most originate in the sacrum, followed by the skull base and the mobile spine. Morphologically, immunohistochemically and ultrastructurally, chordoma phenotypically recapitulates the normal notochord and it has been postulated that they arise from notochordal rests and benign notochordal cell tumors. A variety of chromosomal abnormalities have been identified in chordomas, however, there is little CGH data on chordomas.

Design: Frozen tumor was obtained from 17 chordomas. H&E slides of each tumor sample was analyzed to ensure a high proportion of tumor cells. Genomic DNA was extracted from frozen tissue using the Gentra Puregene isolation kit. We analyzed tumor genome-wide copy number alterations using array comparative genomic hybridization (array CGH). Agilent 244k oligonucleotide arrays were hybridized with tumor DNA labeled in CY5 and control normal DNA labeled in CY3. Signals were captured using an Agilent microarray scanner, and data analyzed using CGH analytics software. High-quality copy number data was produced for all tumors, with copy number gains or losses defined as \log_2 ratios of greater or less than 2 standard deviations. Based on the CGH results immunohistochemical stains for p16 were done on 12 additional chordomas to determine if there was loss of expression.

Results: The patient population ranged in age from 41 to 83 (average 59) years. The tumors were all conventional chordomas by light microscopy and were located in the sacrum, skull base and mobile spine. By CGH the most common abnormality was loss of 1p that was found in all tumors. Loss of 9p (CDKN2A; p16) or chromosome 9 was identified in 15 out of 17 (88%), tumors with homozygous deletion in four tumors. Other common changes included losses of 3p, 4, 10, 13, 14, 18, and 22. Gains were rare and included gains of chromosome 7 (3/14) and 19p (4/14). Immunohistochemical stain for p16 showed no staining in any of the tumors.

Conclusions: Various but overall consistent chromosomal abnormalities are present in chordomas. Frequent loss of 1p and 9p suggest the presence of a tumor suppressor genes that might be important in the pathogenesis of chordoma. The results suggest that p16 is a candidate tumor suppressor gene involved in the pathogenesis of chordoma.

79 Immunohistochemical Expression of Dicer in Soft tissue Sarcomas: Association with Prognostic Significance

DJ Papachristou, A Palekar, J McDavid, D Bartlett, MA Goodman, UNM Rao. University of Pittsburgh Medical Center, Pittsburgh, PA.

Background: MicroRNAs (miR) are small 18-23 nucleotide-long, non-coding RNAs that regulate vital cellular processes. The generation of mature miR from pre-miR, is mediated by a RNase III-related endonuclease, called Dicer. Dicer altered expression is associated with poor survival in several carcinomas. Nonetheless, the expression and

function of this enzyme has never been studied in human mesenchymal neoplasms. Herein, we investigate the expression of Dicer in a panel of soft tissue tumors (STT) and tested its association with clinicopathologic parameters including survival.

Design: Our study was approved by the University of Pittsburgh Institutional Review Board (IRB: 612060). Totally 142 STT (40 benign, 102 malignant [73 high-, 29 low-grade]) as well as reactive and normal tissues were used for the construction of two TMAs. Follow-up data: mean follow-up period=37.6 months, median=33.0, STD=26.2, range=1-115 months. Standard immunohistochemistry was applied (anti-Dicer antibody, Clonogene, Hartford, CT, USA). Immunoreactivity was graded on a scale of 1-3 according to the staining intensity.

Results: 1) Dicer cytoplasmic immunoreactivity was observed in 125/142 of the examined neoplasms, but not in normal mesenchymal tissues. 2) Dicer expression levels were significantly higher in malignant compared to benign and in high- compared to low-grade tumors (Kendall's t , $p < 0.0001$, for all). 3) Augmented Dicer levels were significantly and positively correlated with metastatic potential and patients' death (Kendall's t , $p < 0.005$, for all). 4) Increased Dicer immunoreactivity, elevated tumor grade and size > 5 cm correlated with increased metastatic potential ($p < 0.005$) and worse overall survival (Kaplan-Meier, $p = 0.0005$, 0.004 and 0.017 , respectively). 5) Dicer expression and tumor size, were independent predictors of poor outcome (COX analysis, log-rank $p = 0.003$ and 0.005 , respectively).

Conclusions: 1) Dicer is widely expressed in human STT. 2) Abnormal Dicer expression in soft tissue sarcomas (STS) suggests that miR machinery might be implicated in their pathobiology. 3) Dicer can be used for the prediction of STS with increased metastatic potential and poorer survival. 4) Increased Dicer expression might help to predict the efficiency of future RNA interference-based anti-STS therapeutic strategies.

80 An RT-PCR Assay for FFPE Tissue Identifies a New FUS-DDIT3 Gene Fusion in Myxoid Liposarcoma

MP Powers, W-L Wang, VS Hernandez, KU Patel, AJF Lazar, DH Lopez-Terrada. Baylor College of Medicine and Texas Childrens Hospital, Houston, TX; M.D. Anderson Cancer Center, Houston, TX.

Background: Myxoid Liposarcoma (MLS) is an adipocytic tumor with a myxoid background and shares a differential diagnosis with myxoma, myxofibrosarcoma, lipoblastoma, and extraxial myxoid chondrosarcoma. Two translocations, t(12;16)(q13;p11) and t(12;22)(q13;q12), are pathognomonic for myxoid liposarcoma resulting in at least 13 described alternative gene fusions between the *FUS* (16p11) or *EWSR1* (22q12) genes with the *DDIT3* gene (12q13). RT-PCR from formalin-fixed paraffin-embedded (FFPE) tissue can assist in the diagnosis.

Design: 21 FFPE archival samples of myxoid liposarcoma were obtained. Reverse transcription (RT)-PCR was attempted using previously published primer pairs and conditions. Multiple bioinformatics tools (Primer3, Primer-BLAST, BLAST, and PerlPrimer) were used to analyze the previously published primers and to design new, optimized RT-PCR primers for each of the known chimeric transcripts.

Results: Only a fraction of the MLS samples were amplified with previously published primers covering the most common, but not all, described breakpoints. Seven of the unamplified cases had confirmed *DDIT3* rearrangements by fluorescence in-situ hybridization (FISH). Beta-actin amplified readily suggesting the RNA was intact. A first iteration of new primer design amplified 14 of 21 cases, including 5 of the 7 FISH-confirmed cases. Of the 7 negative cases, 5 were from or prior to 2003, had very weak actin amplification and/or had very low levels of RNA extracted. Bioinformatic analysis suggested multiple parameters that may have decreased primer efficiency. These same tools were used to optimize primer design, which resulted in more efficient amplification of the gene fusions in MLS. The first 6 cases tested all gave expected amplification. A larger than expected amplification product was seen in one sample using primers in exon 7 of *FUS* and exon 3 of *DDIT3*. Sequencing revealed a new, undescribed in-frame translocation between exon 9 of *FUS* and exon 3 of *DDIT3*.

Conclusions: Our results highlight the need for optimal assay and primer design when developing RT-PCR tests for FFPE tumor samples with a prominent acellular and myxoid stroma, such as the fusion transcripts characteristic of MLS. Additionally, we identified a new *FUS-DDIT3* chimeric transcript, which needs to be considered in future assay development, diagnosis, and phenotypic characterization of myxoid liposarcoma.

81 Angiosarcoma: Clinical, Pathological, and Molecular Predictors of Disease-Specific Survival in 222 Patients

P Rao, G Lahat, A Dukah, H Halevi, L Xiao, Z Changye, KD Smith, RE Pollock, D Lev, AJF Lazar. MD Anderson Cancer Center, Houston; MD Anderson Cancer Center, Houston; MD Anderson Cancer Center, Houston, United Kingdom.

Background: Angiosarcoma (AS) is a rare soft tissue sarcoma showing endothelial differentiation as indicated by morphology and expression of CD31 (blood), D2-40 (lymphatic), factor VIII and CD34 (both). We sought to identify clinical, pathological, and molecular predictors of AS specific survival.

Design: Medical records of AS patients (n=222) treated at our institution from 1993 to 2008 were reviewed. An AS tissue microarray (TMA; n=70 specimens) was constructed for immunohistochemical analysis of CD31, CD34, Factor VIII, D2-40, pancytokeratin, Ki67, p53, VEGF, c-Kit, EGFR, and AKT signal transduction pathway activators. Univariate and multivariate analyses were employed to establish independent disease specific survival (DSS) factors.

Results: 43 (19%) metastatic and 179 (81%) localized cases were included. Median survival of localized vs. metastatic AS was 49 (range, 2-188) vs. 10 (range, 1-69) months ($p < 0.0001$). Localized AS undergoing complete surgical resection (n=135; 75%) fared better than unresectable disease (n=44; 25%; $p < 0.0001$). Of univariate factors adverse for DSS, tumor size (> 5 cm vs. ≤ 5 cm, $p = 0.01$) and epithelioid histology ($p = 0.008$) remained independent in completely resected tumors on multivariate analysis. Of the biomarkers evaluated by TMA, 92% of tumors expressed at least one endothelial marker (Factor VIII=83%; CD31=80%; CD34=63%; D2-40=43%) with 88% expressing

2 or more markers. 88 % of tumors expressing D2-40 coexpressed CD31, an unusual combination in normal vessels. No endothelial marker clearly associated with DSS. 50% of epithelioid cases showed keratin expression. Increased expression of AKT pathway activators, especially phospho-4EBP1, was associated with disease progression and shortened DSS on multivariate analysis ($p=0.05$).

Conclusions: Tumor size and epithelioid histology are independent predictors of adverse outcome in AS and should be considered in AS-specific staging systems. Unusual patterns and loss of endothelial markers are common in AS, suggesting use of multiple markers in challenging cases and perhaps indicating important biologic characteristics. The presence of highly expressed AKT pathway activators should be further explored for utility as prognostic factors and therapeutic targets.

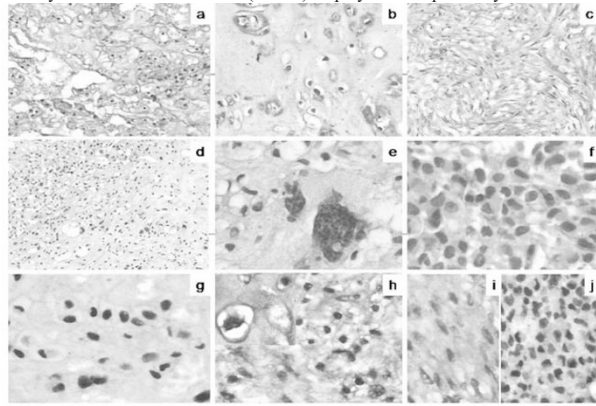
82 Utility of Brachyury as a "New-Age" Marker in the Diagnosis of Chordomas

B Rekhi, K Thorat, NA Jambhekar, R Dikshit, M Agrawal, A Puri. Tata Memorial Hospital, Mumbai, Maharashtra, India.

Background: Brachyury, a nuclear transcription factor, is a recently described immunohistochemical marker to substantiate a diagnosis of a chordoma.

Design: One hundred and four tumors were evaluated for immunohistochemical (IHC) expression of brachyury. These comprised 46 chordomas and 58 other tumors (26 chondroid tumors, 7 liposarcomas, 4 pleomorphic adenomas, 4 mucoepidermoid carcinomas, 4 mucinous adenocarcinomas, 6 germ cell tumors and 2 cases of renal cell carcinoma). Brachyury expression was graded as nil (0), focal nuclear (+), strong (++) and very strong (+++). Only intranuclear (++) and (+++) were regarded as positive. IHC results for CK, EMA and S100 were available in 20 of the 46 chordomas.

Results: The location of chordomas was sacrococcyx in 29 (63%) cases; base of skull in 8 (17.4%) cases and spine in 9 (19.6%) cases. The histology was classical in 33 (71.7%) cases and 11 (23.9%) cases had chondroid matrix. Remaining 1 (2.2%) case, each was labeled as a chondroid chordoma and a de-differentiated chordoma, respectively. Forty out of 46 chordomas (86.9%) displayed positive brachyury staining. While the de-differentiated area in 1 case was negative, the chondroid matrix showed positive staining. None of the 58 other tumors revealed brachyury positivity. The 6 germ cell tumors, including 4 cases of seminoma displayed focal (+) staining, while 1 case, each of embryonal carcinoma and a teratoma, respectively, showed nil staining. Specificity for Brachyury staining in chordomas vs. its differential diagnoses was 100% and sensitivity was 86.9% (CI = 73.7-95.1%). Among the conventional IHC markers, 20 of 20 chordomas (100%) showed CK positivity; 19 of 19 such cases (100%) showed EMA positivity and 16 of 18 chordomas (88.9%) displayed S100 positivity.



a. A classical chordoma with physaliferous cells in a myxoid matrix. b. Chondroid chordoma. c. Areas of spindle cell differentiation in a classical chordoma. d. De-differentiated chordoma. e. Areas of de-differentiation with sarcomatous cells. f. "Plump", eosinophilic cells in a classical chordoma with a solid pattern. g. Positive brachyury expression in a classical chordoma. h. Positive brachyury expression in a chondroid chordoma. Inset showing positive nuclear staining in the chondroid cells. i. Positive brachyury staining in spindle cells in a classical chordoma. j. Positive brachyury expression in "plump" cells in a classical chordoma with a solid pattern.

Conclusions: Brachyury is a single, fairly specific "new-age" marker to substantiate a diagnosis of a chordoma, including its variants. We observed its negativity in lesions which usually form its differential diagnoses. Only strong, intranuclear positivity should be interpreted as positive staining.

83 Massive Localized Lymphedema: A Series of 8 Cases

J Rock, W Wang, WQ Zhao, H Iwenofu, G He. Ohio State University Medical Center, Columbus, OH.

Background: Massive localized lymphedema (MLL) is a benign lesion that clinically and morphologically may simulate well-differentiated liposarcoma. We report a series of 8 cases of MLL and analyze its clinical, morphologic, and immunohistochemical features.

Design: Eight cases from 7 patients were diagnosed MLL and treated in our institution between 2002 and 2008. Clinical history and imaging studies were collected. Surgical specimens were grossly and microscopically examined.

Results: MLL was diagnosed in 7 patients, 5 males and 2 females, aged 23 to 69 years (mean 44). All patients were obese, 3 had hypothyroidism and heart disease, 1 diabetes, and 1 trauma with recurrent lesion. Five MLL occurred at the medial thigh, 2 (male) at the pubic area. All MLL were pre-surgically diagnosed by clinician except one termed suspicious for liposarcoma by radiologist. Grossly, all specimens (1.5-25.7 kg) showed thickened peau d'orange-like skin with tan-yellow, lobulated, focally fibrotic, and markedly edematous cut surfaces. No necrosis or hemorrhage was noted. Histologically, the skin was thickened with mild hyperkeratosis and edematous or hyalinized dermis. The dermis and subcutis showed numerous small to medium-sized, irregularly shaped lymphatic vessels and small, thick-walled blood vessels surrounded by scattered to

dense lymphocytes. One case showed focal dense follicular lymphoid aggregates with germinal centers. The stroma was extremely hypocellular and edematous. Mildly hyperchromatic fibroblasts were present in the stroma or fibrotic septae, but no atypia nor mitotic figures were seen. Lymphocytes were mainly CD4+ T cells, with few CD8+ T cells and B cells, while the case with dense lymphoid follicles showed both dense T and B cells. D2-40 highlighted all the lymphatic channels in dermis/subcutis, while endothelial and smooth muscle markers were positive on blood vessels (less on lymphatic vessels). CD34 was also focally positive on stromal fibroblastic cells. Bcl-2 was positive on some lymphocytes, but negative on stromal cells. Cytokeratin, WT-1, CD99, p53, S-100, and CD68 were all negative. Ki-67 was negative or less than 2% in stromal cell nuclei.

Conclusions: MLL is a benign, reactive, superficial pseudoneoplastic lesion seen in obese patients, displaying marked edema of the dermis and subcutis, numerous distended lymphatic vessels, and small-caliber, round, thick-walled blood vessels often surrounded by infiltrates of T lymphocytes. Lack of nuclear atypia, atypical mitotic figures, and lipoblasts differentiate this lesion from well-differentiated liposarcoma.

84 Balanced and Unbalanced Rearrangement of Chromosome Arm 6q in Chondromyxoid Fibroma (CMF): Delineation of Breakpoints and Analysis of Candidate Target Genes

S Romeo, RAJ Duim, F Mertens, D De Jong, P Dal Cin, M Debiec-Rychter, R Sciot, A Rosenberg, K Szuhai, PCW Hogendoorn. Leiden University Medical Center, Leiden, Netherlands; Lund University Hospital, Lund, Sweden; Brigham and Women's Hospital, Boston, MA; Catholic University of Leuven, Leuven, Belgium; Massachusetts General Hospital, Boston, MA.

Background: CMF is a benign cartilaginous tumour of bone mainly occurring in the second decade of life in long bones. Recurrent rearrangements of chromosomal bands 6p25, 6p23-25, 6q12-15 or 6q23-27 are reported. We aimed to refine location and functional consequences of these rearrangements.

Design: Structural chromosomal aberrations were studied in 7 cases, including 5 not previously reported, by CoBRA-FISH and conventional G-banding. Breakpoints FISH mapping was performed in case L1788. Array CGH was performed on 15 cases to identify additional copy number changes. On the basis of the results 14 cases were further evaluated by interphase FISH. The expression level of candidate genes close to the breakpoints was studied by immunohistochemistry and Q-PCR in 25 and 15 cases, respectively.

Results: The karyotypes in the 5 new cases were:

Number	Description
L1788	46,XX,t(6;17)(q23;p13)
L2367	46,XY,der(6)(6qter->6q27::6p27->6q13::6q27->6q27::6q13->6qter), del(6)(q13), der(22)t(6;22)(q24;p11)
L2499	46,XY,del(6)(q27?1), -13,der(?)t(?)1?(q12)
L2514	46,XY,del(6)(q15q23),del(6)(q173q275),add(11)(q275)
L2515	46,XY,der(6)t(6;10)(p25;p11)t(6;11)(q24;p12),del(6)(q12), der(10)t(6;10)(q12;p11),der(11)t(6;11)(q24;p12)

The other two showed: 46,XY,del(6)(q15),der(6)t(6;6)(q15;q27)inv(6)(p25q13) (L1787); 46,XX,del(6)(?q21?q23),add(7)(q21) (L1789). No copy number changes was found in 12 cases, including L1788, L2367, L1787 and L2515. A small overlapping deletion on 6q24, in the region of *UTRN*, was found in 4 cases, including L1789 and L2499. FISH mapping showed possible involvement of *BCLAF1* on 6q23. No significant expression impairment of these two tumor suppressor genes was found in the evaluated series.

Conclusions: The present study confirmed the nonrandom involvement of chromosome arm 6q in CMF. Both balanced and unbalanced recurrent rearrangements were detected and candidate genes were studied. These data indicate that multiple genes in chromosome 6 are involved in the pathogenesis of CMF.

85 Balanced Rearrangement of Chromosome 5 and 17 in Chondroblastoma: Hints for Its Pathogenesis

S Romeo, K Szuhai, I Nishimori, M Ijszenga, P Wijers-Koster, PCW Hogendoorn. Leiden University Medical Center, Leiden, Netherlands; Kochi Medical School, Kochi, Japan.

Background: Chondroblastoma is a benign cartilaginous tumor of bone predominantly affecting the epiphysis of young males. Conventional cytogenetics has shown no recurrent chromosomal re-arrangements, so far. We have identified an index-case with a balanced translocation and further investigated the involvement of candidate regions/genes in a cohort of chondroblastomas.

Design: CoBRA-FISH karyotyping followed by FISH mapping of the breakpoints using BAC/fosmid clones were performed on the index case. Tumor DNA was isolated and hybridized on BAC array-CGH. Candidate regions were subsequently investigated in 15 chondroblastomas by breakpoint specific FISH probes. Expression of candidate genes was verified by immunohistochemistry in 14 extra cases.

Results: A translocation t(5,17)(p15,q22-23) was found. By array CGH no additional copy number changes were observed in the index-case confirming the balanced nature of the observed translocation. By using breakpoint specific interphase FISH, re-arrangement was found only in the index case and not in other 14 chondroblastomas. The breakpoint in 5p15 was proximal to steroid reductase 5 alpha1 (*SRD5A1*) gene region. Diffuse expression of the protein, as identified by immunohistochemistry, was found in the index case as well as in all other chondroblastomas. Similar pattern of expression was found also for the other sex-steroid signaling-related molecules: estrogen receptor alpha, estrogen receptor beta, androgen receptor and aromatase. The breakpoint in 17q22-23 was proximal to carbonic anhydrase X (*CA10*) gene region with a possible involvement of gene transcription regulatory element. Down-regulation of ca10 protein, as identified by immunohistochemistry, was found in the index-case only.

Conclusions: We report a novel t(5,17)(p15,q22-23) in chondroblastoma without alterations of any of the two chromosome regions in other cases. Diminished expression of CA10 protein -member of the carbonic anhydrase family possibly involved in calcification and bone resorption- was observed in the index case. Impairment of this gene is hypothesized to be relevant for chondroblastoma pathogenesis. Furthermore we observed diffuse expression of SRD5A1. This enzyme is involved in metabolism of testosterone and progesterone. Its diffuse expression confirms the crucial role of sex steroid hormones in cartilaginous tumors.

86 Low Mitotic Rate Does Not Predict Adverse Long Term Outcome in Peripheral Nerve Sheath Tumors

S Sheth, M Bhasin, C Magyar, F Eilber, S Dry. UCLA, Los Angeles, CA.

Background: Increased cellularity (IC), low mitotic rate (MR), and nuclear atypia (NA) are described features of low grade malignant peripheral nerve sheath tumors (MPNSTs). However, specific criteria remain elusive. The clinical significance of low MR in neurofibromas (NFs), especially with other atypical features such as IC or NA, is not well established. Herein, we present the largest known series of PNSTs with low MR and extended clinical follow up.

Design: Materials from 14 patients diagnosed with either low grade MPNST or NF with mitotic activity (PNSTmit) were analyzed. For comparison, we studied 5 high grade MPNSTs and 7 NFs without mitoses (NFno). All had clinical follow up data. Proliferative indices (max. MR/50 HPFs, Ki-67, p53), NA, and cellularity were noted. Maximum MR/50HPF on H&E or PHH3 staining was used. Cellularity, Ki-67 and p53 indices were estimated and also quantified by automated image analysis software. Tumors with >10% p53 nuclear staining were classified as positive.

Results: Fourteen patients (9F,5M), 33-72 years old (mean 47) with tumors 2.0-15.5 cm in size (mean 5.1 cm) comprised the PNSTmit group. Neurofibromatosis type 1 (NF1) affected 5; one patient with a plexiform NF lacked a definite diagnosis of NF1. All had conservative excision and 4 patients, 2 of which had positive margins, received post-operative radiation. All tumors contained mitoses ranging from 1-6/50 HPFs. The mean Ki-67 rate was 1.3% (0.1-5.2%). All tumors were p53 negative. Twelve tumors had NA (5 diffuse) and 10 had IC. NA included pleomorphism, increased size, and dark smudgy chromatin. No aggressive local recurrences (LR) or distant metastases (DM) were seen during a mean 42 months of follow up (range 8-156). One NF1 patient with positive margins had a histologically similar LR at 156 months. There were no significant differences in clinical features, Ki-67, or p53 between the PNSTmit and NFno groups (two way ANOVA). In contrast, 5 high grade MPNSTs had significantly higher MR (mean 184/50 HPF, range 158-295/50 HPF) and Ki-67 rate (20.9%, range 7.5-36.7%) than PNSTmit or NFno (both p<0.001 on 2 way ANOVA). Four MPNST patients had LRs and 2 developed DM; one patient died of disease, one is alive with disease, and 3 are without disease (mean 29 months follow up; range 15-84).

Conclusions: In this series of PNSTs, low MR (<6 mitoses/50 HPF) was not associated with aggressive clinical behavior, even in the setting of IC, NA, or NF1. A low Ki-67 rate (<5%) was seen in all tumors. Longer follow up and additional cases will be needed to confirm our findings.

87 Gene Copy Number Abnormalities Detected by FISH in Soft Tissue Tumors Typically Associated with Recurrent Fusion Proteins

LM Sholl, P Dal Cin, CR Antonescu, CD Fletcher. Brigham and Women's Hospital, Boston, MA; Memorial Sloan-Kettering Cancer Center, New York, NY.

Background: Recurrent chromosomal translocations are common cytogenetic aberrations in soft tissue tumors, and as such have become reliable diagnostic tools. In practice, tumor karyotype is often not routinely performed and we may rely on FISH for detecting specific gene rearrangements. Occasionally, tumors with classic morphology lack the expected rearrangement by FISH but instead show copy number changes of the probed locus. Aside from a few well-described examples, including amplified tumor genes forming rings in dedifferentiated liposarcoma and DFSP, copy number abnormality is not a well-recognized mechanism of tumorigenesis in sarcomas.

Design: We retrieved ten cases that were found to have copy number changes by FISH, including four cases of low grade fibromyxoid sarcoma (LGFMS), one case of extraskeletal myxoid chondrosarcoma (EMCS), three cases of myxoid liposarcoma (MLS), one case of infantile fibrosarcoma, and one case of angiomatoid MFH (AMFH). All cases were reviewed by two soft tissue experts. FISH for FUS, EWS, ETV6, and CHOP was performed on 50 micron paraffin-embedded tissue sections using commercially available break-apart probes.

Results: Four cases of LGFMS contained 3-4 copies of the FUS gene without evidence of rearrangement. One case of AMFH contained 3-4 copies of FUS and centromeric 16 without evidence of rearrangement. One case of infantile fibrosarcoma contained 3 copies of ETV6 and centromeric 12 without evidence of rearrangement. One case of MLS contained 3 to 8 copies of CHOP without evidence of rearrangement. One case of EMCS contained 3-5 copies of the rearranged EWS gene by FISH. Two cases (both high grade myxoid liposarcoma) demonstrated high level amplification: one case contained an amplified CHOP-EWSR1 fusion gene and the other showed amplification of the region of 12q containing CHOP.

Conclusions: A subset of sarcomas with classic morphology lacks the expected underlying translocation but instead harbors copy number alterations of one of the predicted fusion gene partners. Polysomy or amplification involving the fusion gene can also occur and may be dependent on tumor grade. The significance of this observation is unclear but it may potentially cause diagnostic confusion.

88 Methylthioadenosine Phosphorylase and Activated Insulin-Like Growth Factor 1-Receptor: Potential Therapeutic Targets in Chordoma

JB Sommer, DM Itani, KC Homlar, SJ Olson, GE Holt, HS Schwartz, CM Coffin, MJ Kelley, JM Cates. Duke University Medical Center, Durham, NC; Vanderbilt University Medical Center, Nashville, TN; Vanderbilt Orthopaedic Institute, Nashville, TN.

Background: Chemotherapeutic protocols are largely ineffective against chordoma. Advances in targeted molecular therapy, coupled with increased understanding of the molecular pathogenesis of chordoma, may be applicable in the systemic treatment of this aggressive disease. Recent studies have reported co-expression of the insulin-like growth factor-1 receptor (IGF1R) and its ligand in chordoma, but it is unknown whether this receptor tyrosine kinase is activated. Genetic studies have confirmed deletions of chromosome 9p in a subset of chordomas. One of the genes in this region, methylthioadenosine phosphorylase (MTAP) is an essential enzyme in the purine salvage pathway, and is of potential therapeutic relevance because MTAP-deficient cells are sensitive to inhibitors of de novo purine synthesis, such as pemetrexed.

Design: Archived chordoma samples (23 conventional chordomas, 5 chondroid chordomas, and 1 dedifferentiated chordoma), 2 benign notochordal cell tumors (BNCT), and 3 samples of human notochord (17 to 28 weeks gestational age) were stained for the activated isoform of IGF1R (phosphorylated at Y1161) and MTAP by immunohistochemistry (IHC). Cytoplasmic MTAP staining was scored as either negative (MTAP-deficient) or positive. Phospho-IGF1R was scored as positive if there was any specific membranous staining of tumor cells. Overall and disease-free Kaplan-Meier survival curves were compared using the log-rank test.

Results: Phospho-IGF1R was detected in 48% of conventional chordomas. Activated IGF1R was not observed in chondroid chordoma, BNCT, or fetal notochord. Overall, 38% of chordomas were deficient for MTAP by IHC analysis. Patients with phospho-IGF1R-positive tumors had decreased median disease-free survival (15.2 months vs. 48.1 months for negative tumors, p=0.029). MTAP status did not predict overall or disease-free survival.

Conclusions: A significant subset of chordomas demonstrates activation of IGF1R or loss of a key enzyme in the purine salvage pathway. A tendency toward shorter disease-free interval was noted for chordomas with activated IGF1R. Aberrant signaling cascades and disrupted metabolic pathways in chordoma may represent targets for molecular pharmacotherapy in selected susceptible patient populations.

89 Translocations 12;16 and 12;22 in Pediatric Myxoid/Round Cell Liposarcoma: Prevalence and Distribution

R Streblov, K Perry, M Miettinen, R Alaggio, CM Coffin, AL Folpe, M Nelson, A Dafferner, J Woodard, K Yeh, JA Bridge. University of Nebraska Medical Center, Omaha, NE; AFIP, Washington, DC; University of Padova, Italy; Vanderbilt University, Nashville, TN; Mayo Clinic, Rochester, MN.

Background: Myxoid/round cell liposarcomas (MLPS) are characterized by FUS-DDIT3 [t(12;16)(q13;p11)] or EWSR1-DDIT3 [t(12;22)(q13;q12)] fusions. MLPS arise chiefly in adults 40-60 yrs of age. Within this population, the t(12;16) is present in >90% of MLPS and the t(12;22) in <5%. As a diagnostic aid, and to determine the prevalence/distribution of these translocations in pediatric MLPS, we constructed FISH probe sets that can: 1) be performed on formalin-fixed, paraffin-embedded tissue; and 2) identify potential unusual variant translocations or cryptic rearrangements.

Design: Unstained tissue sections from 62 children/young adults (<22 yrs of age) to include 50 MLPS, 7 pleomorphic MLPS, 1 spindle cell MLPS, 1 pleomorphic LPS, 1 lipoblastoma, 1 atypical lipomatous tumor (ALT), and 1 low grade fibromyxoid sarcoma (LGFMS) were submitted for molecular cytogenetic analysis with the diagnoses blinded to the FISH laboratory. Bicolor FISH was performed on each specimen using commercial and/or custom-designed probes composed of select BAC/cosmid clone cocktails capable of assessing DDIT3, FUS and EWSR1 loci independently or as fused translocations.

Results: A FUS-DDIT3 fusion was observed in 37 (86%) of the 43 fusion positive MLPS and an EWSR1-DDIT3 in 6 (14%). Of note, 2 cases exhibited insertions that were not detectable with the commercially available break apart probes of the insertion recipient loci and could only be accurately classified using the custom-designed spanning probes. Also, 1 case demonstrated a rearrangement of only the DDIT3 locus (suggesting the presence of a DDIT3 variant translocation). Seven MLPS, the pleomorphic and spindle cell MLPS, the pleomorphic LPS, the lipoblastoma and the ALT were negative for rearrangements of FUS, DDIT3 and EWSR1. The LGFMS was positive for a FUS-CREB3L2 fusion.

Conclusions: FISH analysis with these newly designed probe sets is a reliable and specific method of detecting MLPS-associated fusions in routinely processed tissue and it may serve as a diagnostic aid in distinguishing MLPS from other myxoid or adipose tissue tumors. Moreover, these probe sets are capable of revealing cryptic or variant translocations. Lastly, these data also suggest that EWSR1-DDIT3 is more frequent in pediatric than adult MLPS.

90 Prognostic Factors in a Single-Centre Series of 160 Cases of Myxoid/Round Cell Liposarcomas (MRLS)

VP Sumathi, RJ Grimer, D Peake, L-G Kindblom. The Royal Orthopaedic Hospital NHS Foundation Trust, Birmingham, United Kingdom.

Background: MRLS is the second most common subtype of liposarcoma and exhibits a wide spectrum of clinical behaviour. The extent of round cell component is known to influence the outcome, but the cut-of percentage has been widely debated. This study aimed to identify clinical and morphologic prognostic factors.

Design: A long term follow-up data from 160 patients with primary MRLS, surgically treated at our centre were statically analysed for prognostic factors. Histology was reviewed in 130(81%) cases.

Results: The tumours occurred in patients with a median age of 48, had a median size of 11cm and predominantly involved the lower extremities (148/160). 53% (69/130) of the tumours had a round cell component (equal or <5% in 40%, >5% in 60%). Local

recurrence occurred in 12%(19/160), metastatic disease in 33% (52/160) and disease specific 5 and 10 year survivals were 75% and 56% respectively(median follow-up for surviving patients was 6.7 years). In 38/52(73%) patients with metastatic disease, the metastases only involved extrapulmonary sites, particularly the soft tissues. 15 patients who received postoperative radiotherapy for contaminated margins did not develop local recurrence.

Conclusions: Multivariate statistical analysis showed that any round cell component(even 1-5%) in MRLS, age > 50 years and tumour size of > 10cms are associated with increased risk of local recurrence and poorer disease specific survival. Post operative radiotherapy for narrow or intralesional margins decreases the risk of local recurrence.

91 Papillary Hemangioma and Glomeruloid Hemangioma Are Distinct Clinicopathological Entities

AJ Suurmeijer. University Medical Center, Groningen, Netherlands.

Background: Papillary hemangioma was recently defined as a morphologically distinct and benign cutaneous hemangioma showing a predominantly intravascular capillary proliferation within dilated thin-walled dermal blood vessels. Glomeruloid hemangioma is a very rare intravascular capillary hemangioma, that structurally resembles the renal glomerulus, and is regarded to be specific for POEMS (polyneuropathy, organomegaly, endocrinopathy, M-protein, skin lesions) syndrome and/or multicentric Castleman's disease. Given their curiosity and mimicry, the differential diagnosis can be difficult and troubling.

Design: Clinicopathologic features of eleven cases of papillary hemangioma recently published were compared with those of five glomeruloid hemangiomas collected through communication with authors who had previously reported on the entity. Immunostaining for CD34, podoplanin, smooth muscle actin, and collagen IV was performed on five papillary hemangiomas and three glomeruloid hemangiomas.

Results: Morphologically, papillary hemangiomas showed a predominant intravascular growth within one or more ectatic dermal blood vessels. Papillary formations contained pericytes and stromal cells, but few capillaries. Luminal surface endothelial cells contained numerous eosinophilic hyaline globules. Glomeruloid hemangiomas also were dermal intravascular lesions, albeit with a glomeruloid appearance due to the presence of numerous capillary loops. Glomeruloid hemangiomas also contained hyaline globules, but less than found in papillary hemangiomas. Immunostaining for CD34, smooth muscle actin, and, in particular, collagen IV highlighted discriminating features. Thin basement membranes and glomeruloid architecture were typical of glomeruloid hemangioma, whereas papillae with thick mantles of basement membrane-like matrix enveloping stromal cells and pericytes were prominent in papillary hemangioma. Both entities were negative for podoplanin. Clinically, glomeruloid hemangioma – often presenting in a spectrum of multiple cutaneous vascular lesions including cherry hemangiomas - was a hallmark of POEMS syndrome and/or multicentric Castleman's disease, whereas papillary hemangioma presented as an innocent solitary cutaneous hemangioma in the head and neck region of otherwise healthy individuals.

Conclusions: Distinct collagen IV immunostaining patterns in papillary hemangioma and glomeruloid hemangioma should enable pathologists to discriminate between these lesions, which is clinically relevant, because glomeruloid hemangioma may be part of POEMS syndrome.

92 Novel, Cloned Translocation Partner in Ewing Sarcoma Couples Its Function to Oncology

K Szuhai, M IJszenga, D de Jong, A Karseladze, HJ Tanke, PCW Hogendoorn. Leiden University Medical Center, Leiden, Netherlands; N. N. Blokhin Cancer Research Center3, Moscow, Russian Federation.

Background: Ewing sarcoma (ES) is an aggressive -second most common- bone sarcoma in childhood. Characteristic t(11;22)(-85-90%), or t(21;22)(-5-10%), or rarer variant translocations with involvement of chromosome 22 (-5%) are present. At the gene level the EWSR1 gene fuses with FLI1, ERG or other ETS transcription factor family members. So far no ES has been identified with fusion of the EWSR1 to transcription factors other than ETS.

Design: Using molecular tools such as multicolor FISH, and array-CGH a ring chromosome containing chromosome 20 and 22 was identified in 3 ES cases. The breakpoint was mapped with (fiber-)FISH, and reverse-transcriptase-PCR followed by sequencing of the fusion partners.

Results: Molecular karyotyping showed the translocation and amplification of chromosomes 20q13 and 22q12 regions. Cloning of the breakpoint showed an in frame fusion between EWSR1 and a novel, hitherto unidentified partner gene. The identified partner is a transcription factor that is not member of the ETS transcription factor family.

Conclusions: A new translocation involving EWS has been cloned. The identified transcription factor is not member of the ETS family nor directly observed thus far in oncogenesis. It has diagnostic implications for ES cases with rearrangements of the EWSR1 gene without known ETS partners especially in bone and soft tissue sarcomas diagnosed as Ewing-like sarcoma.

93 Somatic Mosaicism Is Causative in EXT1/2 Negative Multiple Osteochondroma Detected by Tiling Resolution Array-CGH

K Szuhai, J de Jong, JVMG Bovee, I Jennes, W Wuyts, M Wiveger, HJ Tanke, PCW Hogendoorn. Leiden University Medical Center, Leiden, Netherlands; Leiden University Medical Center, Leiden, Netherlands; University of Antwerp, Antwerp, Belgium.

Background: Multiple osteochondroma (MO) (previously known as multiple exostosis) is a skeletal disorder characterized by the presence of bony outgrowths at the epiphyseal region of long bone. Mutations in EXT1 or EXT2 genes have been observed, both, in sporadic and hereditary cases. Approximately in 70-75% of MO cases point mutation

or small deletions of single exons cause the development of the disease. However, in about 15-20% MO, genomic alteration can not be detected implying the potential role of other alteration such as inversion, translocation or mosaicism. The involvement of other genes or the identification of the putative EXT3 gene still awaits investigation.

Design: We have designed a custom-made Agilent oligonucleotide based chip containing 44000 probes with a tiling coverage of EXT1/2 genes and additional 30 genes involved in heparan sulfate biosynthesis. 16 patient samples with confirmed clinic-pathological appearance of MO and negative for mutation in EXT1 and EXT2 when sequenced and MLPA tested were used (in this study). Array hybridizations, scanning, image and data processing were performed according to standard protocols. As control, DNA samples of 5 MO patients with known deletions in EXT1 or EXT2 genes were selected.

Results: In the control samples all deletions detected by MLPA were confirmed by targeted array-CGH. From the 16 samples with previously undetected mutation, a low degree of deletion of the EXT1 gene was detected in two patients. These results indicated the presence of a mosaic deletion in about 10-15% of the blood cell and were confirmed by interphase FISH.

Conclusions: By using a highly sensitive, custom made chip we identified mosaic deletion of the EXT1 gene in 2 out of 16 analyzed MO patients with otherwise negative test results. Here we showed that oligo-array-CGH approach with tiling resolution have better sensitivity compared to either MLPA based detection or sequencing. For the first time somatic mosaicism with large genomic deletions as the underlying mechanism in MO formation was identified. Furthermore, the existence of mosaic mutations, not alterations of other heparin sulfate biosynthesis related genes, has a significant role in the development of MO in patients who are negative for mutation in Exostosins when analysed by MLPA.

94 Utilization of FISH in the Diagnosis of 235 Mesenchymal Neoplasms: An Institutional Experience

MR Tanas, BP Rubin, R Tubbs, SD Billings, JR Goldblum. Cleveland Clinic, Cleveland, OH.

Background: FISH can detect the translocation and amplification of genes in mesenchymal neoplasms. We report our experience with FISH in 235 mesenchymal neoplasms.

Design: We reviewed 235 consecutive soft tissue consults over a 30 month period where FISH was performed. Probes to *EWSR1*, *FUS*, *DDIT3*, *FOXO1A* and the *MDM2* gene region were used. Major morphological patterns included high grade round cell sarcomas (HGRCS; n=67), high grade spindle cell sarcomas (SSS; n=47), and low grade myxoid (LGMN; n=34), melanocytic (MN; n=19), and adipocytic neoplasms (AN; n=20). Forty-eight cases did not fit into the above patterns.

Results: FISH was utilized in 9% of our soft tissue consults. The most useful probes for the aforementioned patterns and their frequency of rearrangement/amplification for diagnostic entities within those patterns are summarized below.

FISH Results by Morphological Pattern and Diagnosis							
PATTERN	DIAGNOSIS						
HGRCS	EWS/PNET N=23	PDSS N=5	ARMS N=6	RMS,NOS N=5	RCLS N=3	DSRCT N=2	NOS N=23
	EWS+ 96%	SYT+ 100%	FKHR+ 66%	FKHR+ 0%	CHOP+ 100%	EWS+ 100%	EWS+ 6%
				EWS+ 0%			SYT+ 0%
							CHOP+ 0%
							FUS+ 0%
							FKHR+ 0%
SSS	SS N=27	MPNST N=7	NOS N=13				
	SYT+ 96%	SYT+ 0%	SYT+ 0%				
LGMN	LGFMS N=11	Myxoma N=4	MFS N=4	MLPS N=5	NOS N=10		
	FUS+ 91%	FUS+ 0%	FUS+ 0%	FUS+ 100%	FUS+ 0%		
				CHOP+ 0%	CHOP 0%		
MN	CCS N=8	Melanoma N=11					
	EWS+ 88%	EWS+ 0%					
AN	Lipoma N=11	WDLPS N=4	DDLPS N=4	PLPS N=1			
	MDM2+ 0%	MDM2+ 100%	MDM2+ 100%	MDM2+ 0%			
	FUS+ 0%	FUS+ 0%					
	CHOP+ 0%						

EWS/PNET=Ewing's Sarcoma/Peripheral Neuroectodermal Tumor; PDSS=Poorly differentiated synovial sarcoma; ARMS=Alveolar rhabdomyosarcoma; RMS,NOS=Rhabdomyosarcoma not otherwise specified; RCLS=Round cell liposarcoma; DSRCT=Desmoplastic small round cell tumor; NOS=Not otherwise specified; SS=Synovial Sarcoma; MPNST=Malignant peripheral nerve sheath tumor; LGFMS=Low grade fibromyxoid sarcoma; MFS=myxofibrosarcoma; MLPS=myxoid liposarcoma; CCS=clear cell sarcoma; WDLPS=Well-differentiated liposarcoma; DDLPS=Dedifferentiated liposarcoma; PLPS=Pleomorphic Liposarcoma

Conclusions: FISH (using paraffin-embedded tissue) is a frequently utilized sensitive and specific tool for the diagnosis of soft tissue sarcomas, allowing one to distinguish between entities with overlapping morphologic and immunohistochemical features, which often have implications for treatment and prognosis (SS vs. MPNST, CCS vs. metastatic melanoma, lipoma vs. WDLPS, etc.).

95 Intraneural Perineurioma. FISH Assessment of the BCR Locus in 7 Cases

R Tirabosco, S Hing, T Carlstedt, AM Flanagan. Royal National Orthopaedic Hospital, Stanmore, United Kingdom; University College London, London, United Kingdom.

Background: Intraneural perineurioma (IP) is a rare tumor characterized by intraneural neoplastic proliferation of cells showing perineural differentiation. It belongs to a spectrum of tumors comprising the more common soft tissue perineurioma (STP). Despite the different morphology, STP and IP share the immunohistochemical and ultrastructural features. As a group, perineurial cell tumors exhibit chromosomal abnormalities mainly of the 22q11-12 region, involving the BCR and NF2 loci. These loci encode for tumor suppressor genes involved in the pathogenesis of the related meningioma and in a subset of schwannomas. Most genetic studies have been done on STP and only 3 cases of IP have been reported. To assess the frequency of the 22q region abnormalities in IP, we performed FISH on our series.

Design: Seven cases of IP have been retrieved. Typical morphology, diffuse EMA positivity and negative S100 expression, were the criteria for inclusion. Interphase FISH was performed on paraffin sections using a combination of 2 probes on chromosome 22: BCR probe on 22q11.2 and a 22q telomere probe. As a control group, a tissue microarray of 56 neurofibromas has been analyzed.

Results: Summary of clinico-pathological features and FISH are shown in the table 1 and 2. In 2 cases FISH was not informative for technical reasons. All neurofibromas had normal (diploid) copy number of BCR.

Table 1

Case	Sex	Age (y)	Nerve of origin
1	M	51	ulnar
2	M	36	brachial plexus
3	M	33	median
4	F	14	tibial
5	F	17	common peroneal
6	F	36	sciatic
7	M	12	sciatic

Table 2

Case no.	No. of nuclei with BCR loss NN [%]	No. of nuclei with BCR and Telomere loss NN [%]	Total no. of nuclei with BCR loss NN [%]
1	11 [22]	2 [4]	13 [26]
2	8 [16]	17 [34]	25 [50]
3	0 [0]	8 [16]	8 [16]
4	14 [28]	6 [12]	20 [40]
5	6 [12]	14 [28]	20 [40]

NN: number of nuclei with copy loss. 50 nuclei were counted.

Conclusions: Our study, the first of its kind from a single Institution, provides evidence that the majority of IP harbor chromosomal aberration at chromosome 22, either as true monosomy or as part of deletion of genetic material from 22q11-12. Because of the reported close functional relationship between BCR and NF2 genes, it is possible that both tumor suppressor genes are involved in the pathogenesis of perineurial cell tumors. We are currently investigating the loss of heterozygosity status of NF2 in IP, in order to provide a more complete assessment of the 22q11-12 region abnormalities in these tumors.

96 Prognostic Significance of c-Myc Expression in Soft Tissue Leiomyosarcoma

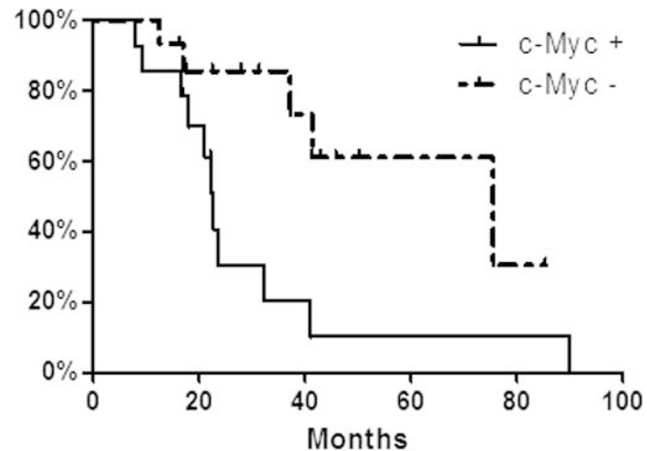
AC Tsiatis, ME Herceg, SJ Olson, HS Schwartz, GE Holt, JM Cates. Johns Hopkins University, Baltimore, MD; Vanderbilt University Medical Center, Nashville, TN; Vanderbilt Orthopaedic Institute, Nashville, TN.

Background: Decreased expression of integrin $\alpha 7$ has been correlated with shorter disease-free survival in soft tissue leiomyosarcoma (LMS). However, use of this marker in routine surgical pathology practice is precluded by the lack of a commercially available antibody for use on formalin-fixed, paraffin-embedded tissue. Other recent data has implicated the oncogenic nuclear transcription factor c-Myc as a direct inhibitor of integrin $\alpha 7$ gene expression. Therefore, we determined whether c-Myc might be a surrogate prognostic marker for decreased integrin $\alpha 7$ expression in LMS.

Design: Immunohistochemical stains for c-Myc were performed on 29 cases of high-grade soft tissue LMS. Tumors were scored as positive for c-Myc expression if >10% of lesional cells demonstrated specific nuclear staining. Comparison of Kaplan-Meier overall and disease-free survival curves was performed using the log rank test. Other clinicopathologic parameters (patient age, sex, tumor size, AJCC TNM stage, and p53 status) were compared using standard univariate statistical methods.

Results: 14 of the 29 LMS samples (48%) were positive for nuclear c-Myc staining. Overall survival for patients with c-Myc-positive tumors (median 22.7 months) was significantly decreased compared to patients with c-Myc-negative tumors (median 75.5 months; $p=0.015$). C-Myc positivity was also associated with shorter disease-free survival (median 8.8 months, compared to 25.1 months for c-Myc-negative tumors; $p=0.006$). C-Myc status did not correlate with patient age, sex, tumor size, AJCC TNM stage, or p53 status.

Overall Survival of Soft Tissue Leiomyosarcoma Patients



Conclusions: Detection of nuclear c-Myc in soft tissue LMS predicts decreased overall and disease-free survival. These results are consistent with previous experimental data showing poor outcomes in LMS patients with decreased integrin $\alpha 7$ expression, since c-Myc inhibits transcription of this integrin gene. Thus, c-Myc status may be a useful prognostic marker and potential therapeutic target in soft tissue LMS.

97 Hemangioendothelioma and Angiosarcoma of Bone: Distinct Histological Criteria Predicting Clinical Behavior

SL Verbeke, F Bertoni, P Bacchini, R Scoti, BJ Mertens, HM Kroon, PC Hogendoorn, JV Bovee. Leiden University Medical Center, Leiden, Netherlands; Rizzoli Institute, Bologna, Italy; University Hospitals, Leuven, Belgium.

Background: Vascular tumors of bone are rare and represent less than 1% of the primary malignant bone tumors. Today, angiosarcoma is the most accepted term for obvious high-grade tumors. However, the existence of an intermediate category is controversial and not recognized by the 2002 WHO classification.

Design: We studied 80 vascular tumors of bone (74 patients), other than hemangioma of bone, diagnosed between 1964 and 2007. All clinical, radiological, and pathologic data were reviewed. Different immunohistochemical and morphological parameters were assessed and related to outcome.

Results: Tumors were positive for CD31 in 67/71 (94%), CD34 in 38/73 (53%), von Willebrand Factor (vWF) in 58/71 (82%), and keratin in 51/73 (70%), although only 18 showed epithelioid phenotype. Multivariate analysis identified two prognostic groups. Group I, in which the combination of a macronucleolus, 3 or more mitoses per 10 high-power field (HPF) and absence of an eosinophilic infiltrate predicted poor prognosis (death within 18 months). This group represents angiosarcoma of bone. Group II, with a better prognosis (5-year survival of 82.3% and metastatic rate of 8.1%), was characterized by the presence of several small nucleoli, less than 3 mitoses per 10 HPF and the presence of an eosinophilic infiltrate. Group II represents the intermediate category and is therefore best labeled as hemangioendothelioma of bone.

Conclusions: CD31 and vWF are sensitive markers to diagnose vascular tumors of bone. Since keratin positivity is seen in 70%, pathologists should avoid misinterpreting them as metastatic carcinoma. We report well defined histological criteria to distinguish two risk groups of vascular tumors of bone with a significantly different clinical course: I. angiosarcoma of bone, and II. hemangioendothelioma of bone as a category intermediate between hemangioma and angiosarcoma.

98 Haemangiopericytoma of Bone: Real or Imagined?

SL Verbeke, CD Fletcher, P Picci, S Daugaard, HM Kroon, PC Hogendoorn, JV Bovee. Leiden University Medical Center, Leiden, Netherlands; Brigham and Women's Hospital, Boston; Rizzoli Institute, Bologna, Italy; Rigshospitalet, Copenhagen, Denmark.

Background: Haemangiopericytoma (HPC) was first described by Murray and Stout as a soft tissue neoplasm with distinct morphologic features, presumably composed of pericytes. Over the years, it became clear that many tumors could mimic a HPC-like pattern. These days, it is accepted that in soft tissue most lesions diagnosed as HPC in the past are actually solitary fibrous tumors (SFT), synovial sarcomas (SS) or myofibromatosis. It has been unclear whether the very rare HPC of bone is a true entity, or that the HPC-like vessels are non-specific and part of other, different entities.

Design: We collected 10 primary HPC of bone from 4 institutions diagnosed between 1952 and 2002. All clinical, radiologic and pathologic data were reviewed. Immunohistochemistry was performed for CD31, CD34, factor VIII, SMA, keratin AE1/AE3 and EMA.

Results: There were 5 female and 5 male patients between 21 and 73 years of age (mean 45.3). All tumors were located within bone. The primary site of the tumor was the femur in two patients, humerus in one, fibula in one, sacrum in two and vertebra in three. All tumors showed the presence of prominent thin-walled branching vessels surrounded by more undifferentiated spindle or round cells. However these cells showed some variation in their morphologic pattern: 5 tumors showed a patternless architecture and varying cellularity, consistent with SFT. Three tumors showed more densely packed sheets of poorly differentiated cells, similar to SS, and 1 case each represented paraganglioma and PEComa, possibly metastatic. Tumors resembling SFT showed usually focal to diffuse

staining for CD34. All tumors were negative for SMA. Two tumors more similar to SS showed focal positive staining for keratin AE1/AE3 or EMA (66%). Some tumors showed severe decalcification artefact. None of the 10 tumors show CD31 and factor VIII expression. FISH is performed to study SYT rearrangements.

Conclusions: Our retrospective review of tumors diagnosed as HPC of bone in the past revealed the absence of true pericytic differentiation and the existence of both SFT of bone and SS of bone. Therefore, as in soft tissue tumors, HPC-like features are non specific. Diffuse CD34 staining is helpful to diagnose SFT of bone, whereas focal keratin/EMA staining is suggestive for SS of bone.

99 Chondrosarcomas: Skip Metastasis

W-L Wang, NJ Hilliard, MT Deavers, VO Lewis, AK Raymond. University of Texas MD Anderson Cancer Center, Houston, TX.

Background: Skip metastases (mets) in chondrosarcoma (ChS) are exceedingly rare. However, their recognition is important as they may be missed by radiologists and pathologists and thereby complicate complete tumor removal.

Design: Five cases of ChS with skip mets were retrieved from the pathology files of our institution. The time frame was 1985-2008 and there were a total of over 700 ChS resections. Clinical and radiological information were reviewed. Skip mets were defined as tumors occurring away from the primary tumor in the same site and separated by either normal bone (i.e., intra-medullary skip met) or an articular surface (i.e., transarticular skip met).

Results: The mean age at presentation was 55 years (range: 33 - 77 years). There were 4 males and 1 female. No patient (pt) had a history of multiple enchondromatosis. The majority of primary tumors occurred in the femur (n=4), one tumor arose in the acetabulum. All pts had intra-medullary skip mets. The mean size of the primary tumor was 14 cm (range: 9 - 19.6 cm). Three cases were dedifferentiated ChS. Two cases were conventional ChS, grade 3/3. Four pts had a single skip met. One pt had multiple skip mets within a single bone. The mean size of skip mets was 8.8 mm (range: 1.0 - 25.0 mm) with the mets separated from the primary tumors by 3.6 - 9.0 mm. Two pts died of disease (7 and 50 months); both of these pts had local relapse and lung mets. One of these pts had multiple skip mets. Three pts had no evidence of disease with an average post-operative follow-up of 37 months (range: 24 - 47 months).

Conclusions: Skip mets are exceedingly rare in ChS and can be very small. Although their presence does not necessarily portend a poor prognosis, their recognition is important to assure complete tumor extirpation at the time of definitive surgery for the primary lesion.

100 Intramuscular Myxoma and Grade I Myxofibrosarcoma Are Characterized by Distinct Genetic Alterations and Specific Composition of Their ECM

SM Willems, AB Mohseny, CI Balog, R Sewrajsing, I Briaire, AM Cleton-Jansen, R Scot, CDM Fletcher, AM Deelder, K Szuhai, PJ Hensbergen, PCW Hogendoorn. LUMC, Leiden, Netherlands; University Hospitals, Leuven, Belgium; Brigham and Women's Hospital, Boston.

Background: Intramuscular myxoma and grade I myxofibrosarcoma are mesenchymal tumours characterized by their abundant myxoid extracellular matrix (ECM). They show considerable histological overlap but differ in clinical behaviour. Therefore the differential diagnosis is important but can be challenging.

Design: We investigated the differences in genetic aberrations and composition of the ECM between both tumours. *GNAS1* activating mutations have been described in intramuscular myxoma while till now, no reports are available for myxofibrosarcoma. Activating mutations in *K-RAS*, which might activate cFos in an alternative pathway, have never been studied in either intramuscular myxoma or myxofibrosarcoma. We documented series of intramuscular myxoma (n=10) and grade I myxofibrosarcoma (n=10) cases were karyotyped, analysed for *GNAS1* and *K-RAS* mutations and downstream activation of cFos mRNA and protein expression. Liquid chromatography mass spectrometry (LC-MS) of tumour lysates identified structural ECM proteins, such as collagen I, VI, XII, XIV and decorin, which we validated by immunohistochemistry and qPCR.

Results: Grade I myxofibrosarcoma showed variable, non-specific cytogenetic aberrations in 83.5 % of cases (n=6) reflecting intrinsic chromosomal instability, whereas karyotypes of intramuscular myxoma were all normal (n=7). *GNAS1* activating mutations were exclusively found in 50% of intramuscular myxoma. Overexpression of downstream cFos mRNA and protein was found in both tumours. No mutations in *K-RAS* codon 12/13 were detected. LC-MS revealed many structural proteins in the ECM of grade I myxofibrosarcoma lacking in intramuscular myxoma. Decorin and collagen VI were expressed significantly higher in grade I myxofibrosarcoma compared to intramuscular myxoma at both mRNA and protein level.

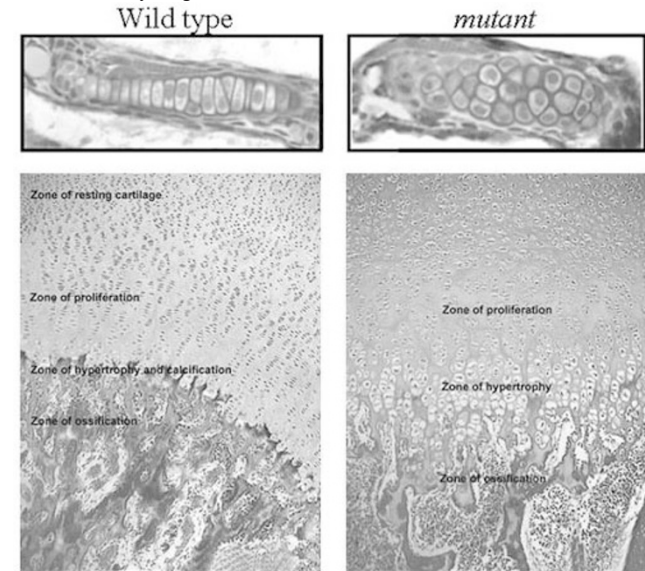
Conclusions: We showed that intramuscular myxoma and grade I myxofibrosarcoma show different molecular genetic aberrations and specific composition of their ECM which probably contribute to their pathogenesis. *GNAS1* mutation analysis can be helpful to distinguish intramuscular myxoma from grade I myxofibrosarcoma in some cases.

101 Zebrafish Model for Studies on Bone Defects in Multiple Osteochondromas

M Wiweger, H Roehl, PCW Hogendoorn. LUMC, Leiden, Netherlands; University of Sheffield, Sheffield, United Kingdom.

Background: Multiple Osteochondromas (MO) previously known as Hereditary Multiple Exostosis (HME) is caused by a mutation in *Exostosins (EXT)* genes, *EXT1* or *EXT2*. MO is characterized by the formation of multiple cartilaginous bone outgrowths near growth plates. However, it seems that MO phenotype is not restricted to osteochondromas. In order to find more information about MO, we use zebrafish mutant called *dackel (dak)* that is mutated in a homologue of the *EXT2* gene. *dak*

mutant is the only available vertebrate that completes embryo development when homozygous for mutation in an *ext* and displays various phenotypical changes e.g. similar chondrocyte organization as this in osteochondromas.



We have recently shown that mutation in *dak/ext2* does not affect cartilage differentiation but it disrupts cartilage morphogenesis and bone development (Clement *et al.*, 2008). As not much is known about bone condition in MO, we examined skeletal changes in juvenile and adult skeletons in *dak/ext2(+/-)* mutants and investigated involvement of FGF signaling in MO.

Design: Zebrafish heterozygous mutants for *dak/ext2*, *ace/fgf8* and their siblings were raised to adolescence, harvested, fixed in 4% PFA and stained with Alizarin red and Alcian blue. Juvenile *dak/ext2* mutants were subjected to TRAP staining. Skeletons were analyzed under dissecting-scope. Each group had minimum 10 fish. Experiments were repeated two times with similar results.

Results: In 20% of *dak/ext2* and *ace/fgf8* mutants deformities similar to those that are well recognized in MO patients i.e. osteochondroma-like outgrowths, bone curving and bone shortening/thickening were found. Similar deformities were also observed in dermal bones, in both zebrafish mutants. TRAP staining indicated altered osteoclast function in *dak/ext2* mutants.

Conclusions: Our findings from zebrafish model indicate that MO patients can have general skeletal problems. Deformities of endochondral bones are more likely to result from malformations of cartilage templates whereas the presence of defects in intramembranous bones is most likely due to osteoclast dysfunction. Similarities between bone phenotype of *dak/ext2* and *ace/fgf8* mutants indicate that impaired FGF signaling might contribute to bone defects in MO.

102 Prognostic Implication of Immunohistochemical Runx2 Expression in Osteosarcoma

KY Won, YW Kim, HR Park, YK Park. Kyung Hee University, Seoul, Republic of Korea; Hallym University, Seoul, Republic of Korea.

Background: Osteosarcoma is the most common primary bone malignancy. Many genetic markers have proven to have prognostic value in osteosarcoma and studies are underway to determine their potential applications as specific therapeutic targets. Runx2, Indian hedgehog (IHH), and Sox9 are proteins that play major roles in bone formation and tumorigenesis. We studied the protein expression of Runx2, IHH, and Sox9 in osteosarcoma and correlated their expression with clinicopathological variables. We also studied the prognostic value of the expression of these three genes in osteosarcoma.

Design: We produced 48 formalin-fixed, paraffin-embedded tissue microarrays containing osteosarcoma tissue cores for immunohistochemical staining of Runx2, IHH and Sox9. We evaluated the expression of each gene by immunohistochemical staining, and analyzed the relationship between expression and clinicopathological parameters.

Results: The high expression of Runx2 was significantly related to metastasis (p=0.015). The high expression of Runx2 indicated a trend toward a poor survival rate (p=0.056). The high expression of IHH and Sox9 were not related to any clinicopathological parameters.

Conclusions: The high expression of Runx2 was significantly related to tumor metastasis in osteosarcoma. Our results suggest that overexpression of Runx2 might be a useful prognostic marker in osteosarcoma cases.

103 Cytogenetic and Molecular Cytogenetic Findings in Chondromyxoid Fibroma: Aberrations of 6q13 Mapped to the COL12A1 Locus by Fluorescence In Situ Hybridization

T Yasuda, J Nishio, KM Kapels, PA Althof, JR Sawyer, JD Reith, JA Bridge. University of Nebraska Medical Center, Omaha, NE; Fukuoka University Chikushino Hospital, Fukuoka, Japan; University of Arkansas, Little Rock, AR; University of Florida College of Medicine, Gainesville, FL.

Background: Chondromyxoid fibroma (CMF), a rare benign bone tumor, may be mistaken for chondrosarcoma. Although cytogenetic studies of CMF are few, rearrangements of the long arm of chromosome 6 frequently expressed as an inv(6)

(p25q13) are prominent. The objectives of this study were to: 1) broaden the currently available cytogenetic data on this unusual entity by subjecting additional CMFs to karyotypic analysis; 2) further localize the recurrently involved 6q13 breakpoint; and, 3) uncover potential candidate gene(s).

Design: 15 CMF specimens from 13 patients were analyzed utilizing standard cytogenetic analysis. A fluorescence in situ hybridization (FISH)-based positional cloning strategy on CMF abnormal metaphase cells using a series of bacterial and P1 artificial chromosome (BAC/PAC) probe combinations spanning a 6.1 Mb region was employed for narrowing the 6q13 breakpoint. Following identification of the BAC/PAC probe sets most closely approximating the critical 6q13 breakpoint, additional FISH studies were conducted on interphase cells obtained from cytologic touch preparations of 12 CMFs.

Results: Chromosome 6 abnormalities were detected in 9 of the 10 clonally abnormal CMFs. In addition to 6q13 rearrangements, recurrent 6p25 and 6q25 anomalies were detected. FISH studies demonstrated that the definitive 6q13 breakpoint locus was flanked proximally by a RP11-560020, RP11-53604 and RP1-238D15 BAC/PAC probe cocktail and distally by a RP11-209D8 and RP1-234P15 BAC/PAC probe cocktail; a region encompassing the *COL12A1* gene locus. Abnormalities of 6q13 were identified by metaphase and/or interphase cell FISH analysis in 2 of 14 (14%) CMFs.

Conclusions: These cytogenetic and molecular cytogenetic findings expand our knowledge of chromosomal alterations in CMF, further localize the critically involved 6q13 breakpoint with identification of *COL12A1* as the likely gene candidate, and provide an alternative approach for detecting 6q13 abnormalities in nondividing cells of CMF. The latter could potentially be utilized as an adjunct in diagnostically challenging cases.

Breast

104 Histologic Grading of Invasive Lobular Carcinoma: Does Use of a Two-Tiered Nuclear Grading System Improve Interobserver Variability?

AL Adams, DC Chheng, WC Bell, T Winokur, O Hameed. University of Alabama at Birmingham, Birmingham, AL.

Background: The Nottingham histologic grade (NHG) is an established prognostic marker for infiltrating ductal carcinoma. Its usefulness in the case of invasive lobular carcinoma (ILC) has been less clear, given that two of the three parameters, tubule formation and mitotic activity, show little variation in ILC, thereby placing much of the emphasis on nuclear grade. We have previously reported a trend for improved overall and relapse-free survival in patients with ILC of low nuclear grade, as classified by a two-tiered nuclear grading system. Given the inherent potential for interobserver variability with any grading system, the goal of the current study is to compare the degree of interobserver variability in the grading of ILC utilizing a two-tiered nuclear grade versus the NHG.

Design: Representative sections from 38 cases of ILC were graded independently by 5 pathologists using NHG criteria for tubule formation, nuclear pleomorphism, and mitotic activity. In addition to the NHG, tumors were categorized by a two-tiered nuclear grading system as low grade (grade 1 nuclei) or high grade (grades 2-3 nuclei). Pair-wise kappa values and interobserver agreement rates were calculated for both the NHG and the nuclear grade, and results were compared using the paired t-test.

Results: Results are summarized in the table. Overall, mean kappa values demonstrated only fair (NHG) to moderate (nuclear grade) agreement. A statistically significant difference was observed between kappa values for NHG compared to those for nuclear grade. Interobserver agreement rates also showed improvement with use of the nuclear grading system as compared to NHG.

	NHG	Nuclear Grade	P Value
Kappa	0.0828 to 0.572 (mean 0.3228)	0.304 to 0.695 (mean 0.4738)	0.0021
Interobserver Agreement Rate	53-79% (mean 70%)	68-92% (mean 83%)	<0.0001

Conclusions: Interobserver variability is to be expected with any histologic grading system. Given that histologic grade has prognostic implications for breast cancer patients which may guide treatment choices, accurate reporting of histologic grade is paramount. In the case of ILC, where use of the traditional NHG places substantial weight on the criterion of nuclear pleomorphism, a two-tiered nuclear grading system may reduce interobserver variability yet still provide useful prognostic information.

105 Molecular Profile of Breast Cancer Metastases to the Central Nervous System

N Alberti, D Val, J Vicens, MF Garijo, JF Val-Bernal, P de Agustin, MJ Merino. National Cancer Institute, Bethesda, MD; Marques de Valdecilla University Hospital, Santander, Spain; "12 de Octubre" University Hospital, Madrid, Spain.

Background: Breast cancer (BC) is the second most common cause of central nervous system (CNS) metastases, developing in 10-20% of patients with BC. Previous studies have suggested that patients with positive HER2 status BC developed CNS metastases within 16 months, thus, development of new molecular therapies that interfere with HER2 pathways are needed. We studied primary tumors and corresponding CNS metastasis of patients with BC to compare the expression of molecular markers (ER/PR, HER2, EGFR) in both locations and to identify molecular profile of primary BC which could indicate an increased risk for spread to the CNS.

Design: Twenty patients with primary BC and their corresponding CNS metastases were studied. Clinical data and pathologic features were reviewed. Treatment of primary BC included surgery, chemotherapy and radiation. All cases were evaluated for estrogens-(ER)/progesterone-(PR) receptors, HER2 and EGFR expression by immunohistochemistry (IHC). HER2 status was also evaluated by chromogenic in situ hybridization (CISH).

Results: Patients had an average age of 47 years (range 27-70years). All primary tumors were invasive ductal carcinomas, of moderate (35%) and high histologic grade (65%). Primary BC show negative ER/PR, positive EGFR and positive HER2 status in 56%, 31%, and 30% of cases respectively. A 56 % of tumors expressed positive EGFR and/or HER2 status with negative ER/PR. CNS metastases had the same ER/PR, EGFR and HER2 status as the primary tumors in 95%, 80% and 95% of cases respectively. In both primary and metastatic lesions, we found high concordance between IHC and CISH in HER2 status testing. All IHC negative (0/1+) and positive (3+) cases were unamplified and amplified by CISH respectively. IHC-equivocal (2+) results were found in 7/40 (17%) samples, corresponding to 5 primary and 2 metastatic tumors. In these cases, CISH confirmed gene amplification in 2 primary lesions and nonamplification in the remaining five tumors.

Conclusions: Our study suggests that patients affected by primary BC with negative ER/PR and positive HER2 or EGFR status are more susceptible to develop metastases to the CNS. Molecular profile of the primary tumor has been maintained in the CNS metastasis.

106 Can We Predict Which Cases of Atypical Ductal Hyperplasia on Breast Core Needle Biopsy Will Upgrade?

KH Allison, PR Eby, J Kohr, WB DeMartini, CD Lehman. University of Washington Medical Center, Seattle, WA; Seattle Cancer Care Alliance, Seattle, WA.

Background: Prior studies suggest atypical ductal hyperplasia (ADH) involving ≤ 2 foci at 11- or 14-gauge stereotactic vacuum assisted breast biopsy (VABB) may not require surgical excision because upgrading to carcinoma does not occur.

Design: Retrospective review of 991 consecutive 9- or 11-gauge stereotactic VABB procedures from February 2001 through June 2006 identified 94 cases performed for mammographic calcifications, confirmed to contain ADH on blinded pathology review. All of these cases had subsequent surgical follow-up. Each large duct or terminal duct-lobular unit containing ADH was counted as a focus and the total number of foci were determined for each case. The largest span of contiguous ADH was measured. The presence of a micropapillary growth pattern or findings suspicious for DCIS was noted. Pathology reports of the excisional biopsy specimens were reviewed to determine which cases upgraded.

Results: Fifteen of 94 (16%) cases of ADH upgraded to carcinoma on excision (13 DCIS, 2 invasive). Cases with > 2 foci were significantly more likely to upgrade (12 of 51 upgraded, $P=0.045$, Fisher's exact test), but the risk of upgrade for cases with ≤ 2 foci was 7% (3/43). The greatest diameter of ADH in the 15 cases that upgraded ranged from 0.2-5.0 mm with 27% measuring ≤ 1.0 mm. The subjective interpretation of "suspicious for DCIS" was a significant predictor of upgrade with 35% (8/23) of cases categorized as suspicious upgrading compared to 10% (7/71) of cases that were not called suspicious ($P=0.008$). Micropapillary features were noted in 10/15 (67%) cases that upgraded compared to 35/79 (44%) cases that did not upgrade but the result did not reach statistical significance.

Conclusions: The risk of upgrade of ADH is associated with the number of foci involved and subjective suspicion for DCIS. However, upgrade at surgical excision can occur even when ≤ 2 foci of ADH are found at VABB. A standardized method of reporting ADH could be used to assess individual patient risk of upgrade and make recommendations for surgical excision.

107 Florid Lobular Intraepithelial Neoplasia (FL-LIN) with Signet Ring Cells (SRC), Central Necrosis and Calcifications: A Clinicopathologic and Immunohistochemical Analysis of Ten Cases

I Alvarado-Cabrero, R Valencia-Cedillo, S Barroso-Bravo. Mexican Oncology Hospital, Mexico, DF, Mexico.

Background: In the most florid type of ductal involvement, LIN proliferates to form a solid mass of tumor cells that fill and expand the duct lumen. Foci such as these can develop central necrosis and calcifications, which are detectable on mammograms. The immunohistochemical expression of E-cadherin has been found to be absent in virtually all reported examples of LIN with necrosis. FL-LIN with necrosis may consist of classical or pleomorphic cell types. However, the occurrence of LIN composed entirely of signet ring cells with central necrosis is extraordinarily rare. We describe herein 10 examples of these cases, to illustrate this uncommon morphologic pattern of Lobular Intraepithelial Neoplasia.

Design: The cases were encountered during routine clinical practice of the authors performed over a 5-year period (2002-2007) at Mexican Oncology Hospital. In all cases, we analyzed the expression of E-cadherin(E), high-molecular-weight keratins (HMWK), Estrogen Receptor (ER), Progesterone Receptor (PR) and Her2/neu. Patient's clinical information was obtained from the medical records.

Results: We reviewed 10 patients with florid LIN with SRC and central necrosis, patient's ranged in age from 45 to 75 years (mean:51.2). Clinical profiles of patients were not significant different from those with classical LIN. The main indications for biopsy were calcifications (n:7) and mass (n:3). On mammography, all calcifications were clustered, punctuate, high density and smaller than or equal to 0.6mm. Luminal necrosis was present in all cases and calcifications in 7 of FL-LIN with SRC. Eight patients (80%) had associated invasive carcinoma including 5 classical lobular, and 3 invasive lobular carcinoma classical type with signet ring cells. Immunoreactivity for ER, PR and HMWK was present in 9/10(90%), 8/10(80%) and 9/10(90%) of cases respectively. All cases had complete absence of staining for E. Overexpression of Her 2/neu was absent in all 10 cases.

Conclusions: Lobular Intraepithelial Neoplasia composed entirely of signet ring cells can develop extreme ductal and lobular enlargement, central necrosis and calcifications. These cases are frequently associated with invasive lobular carcinoma.